Gut protective *Klebsiella* species promotes microbiota recovery and pathobiont clearance while preventing inflammation

Authors: Vitor Cabral[1,*†], Rita A. Oliveira[1,3,*†], Margarida B. Correia[1], Miguel F. Pedro[1,4], Carles Ubeda[2], Karina B. Xavier[1,†]

Affiliations:

[1]Instituto Gulbenkian Ciência, 2780-156 Oeiras, Portugal

[2]FISABIO, Valência, Spain

[3]Current address: Duchossois Family Institute, The University of Chicago, Chicago, IL, USA

[4]Current address: LEAF, TERRA, Instituto Superior de Agronomia, University of Lisbon, Portugal

* These authors contributed equally and share co-first authorship of this publication

[†]To whom correspondence should be addressed:

vcabral@igc.gulbenkian.pt; kxavier@igc.gulbenkian.pt; aaoliveira@uchicago.edu

Keywords: gut microbiota; colonization resistance; probiotic; *Klebsiella*; inflammatory bowels disease; butyrate; inflammation; intestinal pathogens; *Escherichia coli*; AIEC; *Enterobacteriaceae*

Abstract

The microbiota inhabiting the mammalian gut serves as a protective barrier against pathogen invasion through a mechanism known as colonization resistance. Antibiotic treatments can inadvertently disturb the gut microbiota, compromising colonization resistance and increasing host's susceptible to infections. Non-*pneumoniae Klebsiella* spp. members of the gut microbiota play a crucial role in colonization resistance and clearance from the gut of pathogenic *Enterobacteriaceae* following antibiotic-induced perturbations. Specifically, *Klebsiella* strain ARO112 a gut microbiota isolate, can effectively resist and clear *Escherichia coli* colonization after antibiotic-induced dysbiosis.

We assessed the potential of *Klebsiella* sp ARO112 to promote clearance of *Enterobacteriaceae* pathobiont Adherent-Invasive *E. coli* (AIEC) in an Inflammatory Bowel Disease (IBD) mouse model susceptible to inflammatory episodes. In antibiotic-treated IBD-predisposed mice infected with the AIEC, *Klebsiella* sp. ARO112 promoted a faster recovery of gut microbiota members potentially involved in butyrate production and accelerated pathobiont clearance. Functionally, ARO112-driven microbiota recovery promoted higher butyrate levels and prevented intestinal inflammation compared to untreated animals. Conversely, treatment with the well-known probiotic *E. coli* Nissle 1917 enhanced AIEC colonization and inflammation. Furthermore, we assessed the safety of ARO112 as a potential next-generation probiotic; phenotypic comparison of ARO112 against closely related *Enterobacteriaceae* revealed its lower pathogenic potential, including being more recalcitrant to antibiotic resistance acquisition.

Overall, our results showing that *Klebsiella* sp. ARO112 can resolve infections while contributing to the promotion of intestinal health, underscore its potential as a biotherapy agent that can disrupt inflammation-treatment-infection cycles. This potential extends beyond IBD patients, encompassing individuals with other inflammatory-based conditions related to microbiota imbalances.

41 **Introduction**

42 The gut microbiota plays a crucial role in human health and disease. An abundant and diverse
43 intestinal community of microorganisms performs essential functions, including providing colonization
44 resistance to potential pathogenic bacteria[1–4]. This protective capacity can be significantly compromised by
45 environmental perturbations that alter the population composition, such as changes in diet or medical
46 treatments, like antibiotics[5–9]. These shifts in microbial populational dynamics can be challenging to rectify,
47 leaving patients more susceptible to infections and other medical complications[8,10].

48 The pursuit of interventions to restore dysbiotic gut microbiotas has gained momentum. Currently,
49 both basic research and clinical studies encompass a range of approaches, from introducing single protective
50 bacterial species to well-defined bacterial communities or even complete microbiota, as in fecal microbiota
51 transplants (FMT)[11]. Although the United States Food and Drug Administration has recently approved FMT
52 for the successful treatment of recurrent *Clostridioides difficile* infections in humans[12], the undefined nature
53 of these procedures poses safety risks[13,14]. These risks underscore the need for the identification of defined
54 strategies, which could involve either single- or multi-strain bacterial cocktails. Next-generation probiotic
55 bacteria, defined as bacterial species native to the host that upon ingestion and/or colonization provide
56 benefits, offer promise for restoring microbiota functions[15]. This requires an extensive understanding of the
57 benefits, potential drawbacks, and the organism's safety profile, all of which are important to its therapeutic
58 importance.

59 Patients with high susceptibility to infections often undergo extensive antibiotic treatments,
60 rendering them more susceptible to recurrent infections[16,17]. These patients require innovative approaches
61 to complement current treatments and break the cycle of disease recurrence. Inflammatory Bowel Diseases
62 (IBD) are among such diseases where extensive antibiotic treatments can render the patient more susceptible
63 to frequent infections and recurrence of acute disease symptoms[18,19]. IBD are a group of multi-factorial
64 pathologies with a complex etiology, where genetic predisposition, gut microbiota, and environmental
65 conditions play a role[20–23]. Three outcomes emerge as key aspects of disease cycles that afflict IBD patients:
66 gut microbiota imbalances[24], increased and persistent intestinal inflammation[25], and susceptibility to
67 intestinal infections[26]. To manage inflammation flares, IBD patients are often prescribed antibiotics or anti-
68 inflammatory medication[27]. However, these treatment options can inadvertently harm the microbiota, often
69 exacerbating the proinflammatory intestinal environment[16], thus perpetuating the cycle. The consequent
70 loss of natural protection provided by a balanced microbiota often leads to infections by *Enterobacteriaceae*
71 bacteria, like the adherent-invasive *Escherichia coli* (AIEC), which can also trigger inflammatory episodes[28].

72 Probiotics are often considered as potential alternative or complementary treatments for intestinal
73 diseases, but their benefits for complex pathologies like IBD have been limited[29]. The probiotic strain *E. coli*

74 Nissle 1917 (EcN) has been proposed as a potential therapy for IBD[30]. However, despite various proposals
75 and even clinical trials[31], the European Society for Clinical Nutrition and Metabolism, recommends against
76 probiotics for treatment or prevention of Crohn's Disease[32], owing to lack of promising results obtained thus
77 far. Therefore, therapeutic probiotics warrant further research, as their efficacy in patients has been
78 inconsistent[33–36].

79 In previous work, we identified a commensal intestinal bacterium, *Klebsiella* sp. ARO112 from the
80 *Enterobacteriaceae* family[37]. ARO112 provides partial colonization resistance against an invading *Escherichia*
81 *coli* K-12 MG1655 strain and *Salmonella enterica* Typhimurium in a streptomycin-induced intestinal dysbiosis
82 murine model[37]. ARO112 can also partially displace the invader *E. coli*, when administered as a treatment,
83 i.e., after colonization by the invading *E. coli*, in the presence but also in the absence of other microbiota
84 members (in ex-germ-free mice). The ability to displace an already established bacterial invader is not a
85 standard feature, even among probiotic strains. Research has shown that commercially available probiotics
86 can partially displace certain pathogenic bacteria but with varying efficacy[38]. Our previous findings have
87 prompted us to test the potential of ARO112 strain as a next-generation probiotic, capable of eliminating
88 colonization by other *Enterobacteriaceae* invading the gut community during dysbiotic events in a disease
89 model.

90 Here, we assessed the safety of ARO112 strain by evaluating its pathogenic potential for an assembly
91 of pathogenic traits commonly associated with *Enterobacteriaceae* clinical isolates. Our results show that
92 ARO112, compared to other *Enterobacteriaceae,* has low pathogenic potential, including limited efficiency in
93 acquiring or maintaining plasmids carrying antibiotic resistances, and does not induce host inflammation,
94 unlike EcN. Simultaneously, ARO112 displayed a competitive advantage for colonization against different
95 species from the Pseudomonadota phylum (formerly known as Proteobacteria). Its competitive properties
96 and lack of inflammatory potential had a significant impact in an IBD mouse model, where ARO112 exhibited
97 strong potential as a next-generation probiotic, promoting butyrate-producing microbiota recovery from
98 antibiotic-induced dysbiosis, preventing gut inflammation, and reducing infectious AIEC loads, the most
99 common pathobiont in IBD patients[39].

100

101 **Results**

102 **ARO112 encodes fewer predicted pathogenic traits when compared with other *Enterobacteriaceae***

103 To address the safety of ARO112 to be used as a probiotic, we performed a genome comparison
104 analysis with fifteen *Enterobacteriaceae* strains to assess their pathogenic potential, including five *E. coli*
105 strains, five *Klebsiella pneumoniae* strains, and five non-*pneumoniae Klebsiella* strains, including ARO112
106 (Supplementary Table 1). These strains were selected to incorporate human (clinical) and murine bacterial

107 isolates, including pathogenic, commensal, and one established probiotic strain, as well as type or laboratory
108 strains for these groups. With this broad strain selection, we expected to involve a wide range of encoded
109 virulence traits and bacteria with different pathogenic potential.

110 A whole genome-based phylogenetic tree segregates the fifteen strains into three major clades,
111 differentiating among *E. coli*, *K. pneumoniae*, and non-*pneumoniae Klebsiella* strains (Fig. 1a). The non-
112 *pneumoniae Klebsiella* clade shows ARO112 clustering with *Klebsiella grimontii* (Kgr) type strain and close to
113 *K. michiganensis* (Kmi) type strain, and *Klebsiella* MBC022 mouse commensal strain clustering with the *K.*
114 *oxytoca* DSM5175 (Kox) type strain. This placement of ARO112 closer to Kgr than Kmi was recently shown by
115 others[40,41], where phylogenetic analysis with new *Klebsiella* isolates placed ARO112 strain close, but not part
116 of, the cluster containing three *K. grimontii* strains[40]. These results showing that ARO112 is phylogenetically
117 closer to *K. grimontii* than *K. michiganensis*, mean that it can no longer be considered a *K. michiganensis*, as
118 initially classified[37], and raises the hypothesis that ARO112 might be a new species more closely related to *K.*
119 *grimontii*. In the *E. coli* clade, the probiotic EcN and the pathobiont AIEC (LF82) strains were phylogenetically
120 closer to each other than to both non-pathogenic *E. coli* K-12 (MG1655) and *E. coli* B (EcB) laboratory strains
121 and to the clinical isolate *E. coli* (Ec1898) (Fig. 1a). In the *K. pneumoniae* clade, the three clinical isolates
122 cluster together (MH258, Kp1012, and Kp834), while the other two *K. pneumoniae* strains (Kpn NCTC9633
123 and ATCC43816) form a distinct cluster.

124 To predict the genome-encoded pathogenic potential of these strains we resorted to 9 databases,
125 reported in Bacterial and Viral Bioinformatics Resource Center[42], for virulence factors, drug targets and
126 transporters, and antibiotic resistance genes. The presence/absence of the pathogenic properties segregated
127 the three clades represented in the phylogenetic tree (Fig. 1b and 1c). Interestingly, when comparing the
128 ubiquitous gene products and pathogenic properties per clade (shared by the five strains within a clade),
129 there is a higher percentage of gene products that are not ubiquitous to any of the three clades (>75%),
130 compared to the lower percentage of predicted pathogenic traits (<20%) (Supplementary Fig.1).

131 Upon adding data for the abundance of each pathogenic property (Supplementary Table 4), instead
132 of the binary analysis of presence/absence, the strains were no longer segregated by taxonomy, and instead
133 segregated in two clusters along PCo 2 (Fig. 1d). One cluster included a known multi-drug resistant (MDR) *K.*
134 *pneumoniae* strain (MH258) and three strains isolated from hospitalized patients. The top 10 pathogenic
135 traits driving the separation of the two clusters include several antimicrobial resistance-associated properties
136 (6/10; Supplementary Table 5), and accordingly these properties were enriched in the cluster including the
137 MDR *K. pneumoniae* strain. ARO112 was in the second cluster together with MBC022, both isolated from
138 non-antibiotic-treated gut microbiomes, and together with known non-MDR strains like MG1655 (Fig. 1d).

139 To assess the presence of gene products that might have clinical relevance, but not be necessarily
140 included in the available pathogenic properties databases, we analyzed the genomes of each strain for the
141 number of gene products related to the following categories: conjugation, natural competence, multidrug
142 resistance, transposases, phages/integrases, and CRISPR systems. With this analysis, ARO112 consistently
143 shows a lower number of gene products within these categories in comparison with all the other *pneumoniae*
144 and most non-*pneumoniae Klebsiella* strains (Fig. 1e). Importantly, ARO112 was the only *Klebsiella* with no
145 gene products related to conjugation or conjugal proteins, which are important for bacteria to acquire
146 antibiotic resistance genes (Fig. 1e). Moreover, even though the genome analysis displays Kgr as the closest
147 tested relative to ARO112 (Fig. 1a) and the predicted pathogenic traits analysis hints at Kmi as closely related
148 to ARO112 (Fig. 1b), both Kgr and Kmi type strains clearly differ from ARO112 when focusing on gene
149 products for such clinically-relevant categories (Fig. 1e), supporting that ARO112 might have a lower
150 pathogenic potential.

151 Overall, these results show that the predicted pathogenic properties encoded by the different
152 bacteria correlate with the taxonomy. In contrast, the abundance of these properties segregates by the drug
153 resistance-encoded genes of individual isolates, regardless of taxonomy. ARO112 separated from known
154 MDR strain MH258 and clinical isolates Kp1012, Kp834, and Ec1898, and showed overall less predicted
155 pathogenic properties than the ensemble of the other tested strains.

156

157 **ARO112 shows fewer phenotypic traits associated with nosocomial infections**

158 Given that genome predictions do not always directly translate into phenotypes, we decided to
159 perform several in vitro tests for traits that are generally associated with *Enterobacteriaceae* pathogenicity
160 in nosocomial infections and gut colonization (Fig. 2a). For that, we selected a subset of the aforementioned
161 strains, including four *E. coli* strains (non-pathogenic K-12 MG1655 strain, pathobiont AIEC, probiotic EcN,
162 and clinical isolate Ec1898), three *K. pneumoniae* strains (clinical isolates MH258, Kp1012, and Kp834), and
163 two non-*pneumoniae Klebsiella* strains from our strain collection (MBC022, ARO112). We performed these
164 tests under two different laboratory conditions (nutrient rich – LB – and nutrient poor media – M9 salts
165 minimal medium with glucose) to evaluate if these pathogenic traits vary in different environments.

166 We started by testing antibiotic resistances, as this is the main driver of clinical problems associated
167 with *Enterobacteriaceae*[43], due to their efficient ability to acquire and share antibiotic resistance genes from
168 other bacteria through mechanisms like horizontal gene transfer (HGT)[44]. Our results showed that ARO112,
169 like MG1655, EcN, and MBC022, is not MDR since it displays resistance to less than three classes of antibiotics
170 (Fig. 2b). The other five strains tested showed resistance to three classes of antibiotics (AIEC in rich medium)
171 or more than three in both media, including, as expected, the known MDR strain MH258 in addition to the

172 clinical isolates from hospitalized patients Ec1898, Kp1012, and Kp834 (Fig. 2b), supporting their clustering
173 together as predicted MDR strains (Fig. 1d). Most of all, these results confirm that ARO112 is not MDR and
174 highlight that bacterial phenotypes are context dependent, with minimal medium, frequently, potentiating
175 resistance phenotypes.

176 Biofilms are microbial communities enclosed in extracellular matrices and adherent to a substrate,
177 and can contribute to increased recalcitrance to antibiotic treatments[45]. We found that Kp1012 was the strain
178 that produced the most robust biofilm biomass, in minimal medium. In rich medium, most strains resulted in
179 low (EcN, Kp834, MBC022, ARO112) or very low (Ec1898, MH258) biofilm biomass (Fig. 2c), with only
180 MG1655, AIEC, and Kp1012 showing slightly higher biofilm biomass (Fig. 2c). Under minimal medium,
181 ARO112, Kp834, and MBC022 presented some capacity for biofilm formation, but much lower than Kp1012.
182 All *E. coli* strains and MH258 showed lower biofilm biomasses (Fig. 2c).

183 Urease production is a common trait in *K. pneumonia* and *K. oxytoca* and can be problematic in
184 urinary tract infections, whilst it might also be a good competitive trait for gut colonization[46]. In cultures
185 grown in rich medium, there was no detectable urease activity, except for *K. oxytoca* MBC022 and, to a lesser
186 extent, ARO112, both displaying low levels of urease (Fig. 2d). In cultures grown in minimal medium all
187 *Klebsiella* strains, but not *E. coli* strains, showed significantly higher urease activity, with Kp1012 and MBC022
188 presenting the highest and Kp834, MH258, and ARO112 the lowest activities, with the latter displaying similar
189 levels to rich medium (Fig. 2d). The absence of urease activity in the *E. coli* strains is expected, since this
190 species is a known non-urease producer, with only some clinical isolates of the pathogenic
191 Enterohemorrhagic *E. coli* reported to have urease activity[47]. Strains proficient in both biofilm formation and
192 urease production, as is the case for Kp1012, can become problematic and often associated with recurrent
193 urinary tract infections[48].

194 In rich medium, which is not limited in iron, all strains showed a reduced production of iron chelators,
195 siderophores (Fig. 2e). Interestingly, in iron-limiting conditions, siderophore production was not increased in
196 ARO112, MG1655, nor MBC022, as opposed to the rest of the strains, where a significantly higher
197 siderophore production was observed (Fig. 2e), even though growth yield was unaffected for ARO112, when
198 comparing rich and minimal medium (Extended Data Fig. 1a).

199 When testing resistance to serum-mediated killing of bacteria grown in rich medium, only the *K.*
200 *pneumoniae* strains and MBC022 showed significant resistance to and replication ability in the presence of
201 human serum (Fig. 2f), indicating their potential capacity to survive and thrive in the bloodstream of patients.
202 On the contrary, most *E. coli* strains (MG1655, AIEC, EcN) are very susceptible to human serum, while Ec1898
203 and ARO112 are not killed by nor do they replicate in human serum (Fig. 2f). Interestingly, testing these
204 strains grown in minimal medium resulted in a significantly higher replication for MH258, increasing from 40-

205 (in rich medium) to 140-fold. More surprising, however, was the change detected for EcN where we observed
206 a strong serum resistance and replication capacity when grown in minimal medium (70-fold increase; Fig. 2f).
207 Reports on this phenotype are usually performed using rich media to grow bacteria[49,50], but here we found
208 that some bacteria, like EcN and MH258, show increased proliferation when grown in minimal medium.
209 Finally, ARO112 shows no evidence of being killed by the human serum, but neither does it replicate to the
210 levels seen for most strains (Fig. 2f). Since this pathogenic trait directly affects the host, as it potentially allows
211 bacteria to proliferate in the bloodstream, with life-threatening risks, ARO112 inability to proliferate is a
212 desirable trait for a potential probiotic.

213 The evaluation of the pathogenic potential based on phenotypic assays gives us the resolution to the
214 strain level for the pathogenic traits selected. While the genome-based approach showed us that the
215 pathogenic traits predicted to be present or absent in the genome correlate with the taxonomy, the selective
216 testing of clinically-important phenotypes allows us to distinguish distinctly active pathogenic traits within a
217 taxon, such as the heterogeneity within both the *E. coli* and the *K. pneumoniae* clades, but also to pinpoint
218 strains with overall less pathogenic traits associated with nosocomial infections. Notably, ARO112 stands out
219 with low pathogenic traits commonly associated with nosocomial infections.

220

221 **ARO112 is resistant to acquire and retain plasmids bearing antibiotic resistance**

222 The lack of resistance found in the commensal non-clinical strains does not exclude the potential for
223 antibiotic resistance acquisition by HGT, which is common among *Enterobacteriaceae* within complex
224 communities, like the gut microbiota[51,52]. Indeed, the acquisition of antibiotic resistance, in particular by HGT
225 events, has been shown to be problematic, with *Enterobacteriaceae* at the forefront of this increasingly
226 concerning medical issue[44]. Therefore, we assessed the capacity of ARO112 to acquire resistances from donor
227 bacteria through HGT, in comparison with the probiotic EcN and the MDR *K. pneumoniae* strain that had
228 typical phenotypes found in causative agents of nosocomial infections, Kp1012. We tested the transfer of a
229 commonly used conjugative plasmid (RP4) from a donor strain (MG1655 or Kgr) into the aforementioned
230 recipient strains. Interestingly, the already MDR strain Kp1012 had the highest acquisition rate, with a median
231 of 83% and 25% of cells acquiring the plasmid from the MG1655 and Kgr donors, respectively (Fig. 2g). EcN
232 presented an intermediate transfer rate, with a median of 25% and 4% acquiring the plasmid and consequent
233 antibiotic resistance from MG1655 and Kgr, respectively (Fig. 2g). In contrast, ARO112 showed strong
234 resistance to plasmid acquisition, with a median of less than 4% of the population acquiring the RP4 plasmid
235 from MG1655 donor strain, and less than 0.5% from Kgr donor strain (Fig. 2g). Next, we tested the capacity
236 to retain the acquired plasmids, after five days of daily passages in rich or minimal media in the absence of
237 antibiotic selection. Remarkably, ARO112 showed the highest plasmid loss, with 87% and 65% of the

238 population losing the plasmid in rich and minimal media, respectively (Fig. 2h). In contrast, the MDR strain
239 Kp1012 lost the plasmid in 27% and 2% of the population, in rich and minimal media, respectively, and EcN
240 lost the plasmid in 61% and 34% of the population in rich and minimal media, respectively (Fig. 2h).

241 Even plasmids that are non-self-transmissible, can be transferred among bacteria, through
242 conjugation events[53] in which non-conjugative plasmids take advantage of conjugative plasmids' machinery.
243 We have also tested the capacity of ARO112, EcN, and Kp1012 to retain a non-conjugative plasmid
244 (pMP7605) carrying an antibiotic resistance received by electroporation. Kp1012 barely lost the plasmid,
245 both in rich (7%) and minimal media (11%; Fig. 2i), and 42% of EcN colonies lost the non-conjugative plasmid
246 in rich medium (Fig. 2i), while no loss was observed in minimal medium (Fig. 2i). Remarkably, ARO112 showed
247 the highest plasmid loss, with 83% and 51% of the population losing the non-conjugative plasmid when grown
248 in rich or minimal media, respectively (Fig. 2i).

249 Natural plasmids are known to be more stably maintained as they often confer some fitness
250 advantages that drive their persistence (Alonso-del Valle, 2021). We also tested the retention capacity of
251 Kanamycin resistance transferred from one of the MDR clinical isolates predicted to bear natural plasmid(s),
252 Kp834, into ARO112 and EcN (Kp1012 was not tested due to its MDR complicating counterselection). EcN did
253 not lose the resistance, while ARO112 lost the resistance in over 15% (rich medium) and 30% (minimal
254 medium) of the population (Extended Data Fig. 1b).

255 In summary, even though ARO112 shares with other *Enterobacteriaceae* strains the capacity to
256 acquire plasmids, when compared to the probiotic strain EcN and the *K. pneumoniae* clinical isolate Kp1012,
257 ARO112 is much less efficient in plasmid acquisition and retention, a main source of antimicrobial resistance
258 in *Enterobacteriaceae* and, therefore, presents a reduced risk of becoming a clinical problem.

259

260 **Colonization of the murine gut can alter expression of bacterial phenotypic traits**

261 Having observed that the tested phenotypes varied depending on the culture medium used, we
262 questioned which of the tested laboratory media, rich or minimal, was resembling the phenotypical profiles
263 of bacteria in the mammalian gut more closely. Therefore, we tested the phenotypes whose assays do not
264 require bacterial growth, testing directly in bacteria collected from fecal samples of mono-colonized mice
265 (Fig. 3a). We compared the phenotypes of ARO112 with EcN and Kp1012 collected from fecal samples of ex-
266 germ-free mice colonized for five days with each of these bacteria, without selection or growth. Regarding
267 urease activity, Kp1012 presented the same high urease activity detected in minimal medium-grown cultures
268 and EcN showed the expected low urease activity also observed in all laboratory-grown cultures (Fig. 3b and
269 2d); ARO112 presents a variable phenotype, with half the samples showing low urease activity, similar to the
270 results obtained with cultures grown in the laboratory, while the other half showed increased urease activity

271 (Fig. 3b and 2d). This result, while surprising due to the low levels of urease activity in culture-grown ARO112,
272 indicates that in this strain this phenotype is regulated differently in the gut environment. Interestingly, fecal
273 siderophore measurements showed low values for all three strains, but with a similar tendency observed in
274 minimal medium of lower values for ARO112, when compared with both EcN and Kp1012 (Extended Data
275 Fig. 2a and Fig. 2e).

276 When testing for resistance to human serum after gut colonization, similar results were obtained
277 with bacteria extracted directly from feces of mono-colonized mice (Fig. 3c) to the ones of laboratory-grown
278 cultures (Fig. 2f). When compared to both Kp1012 and EcN, ARO112 strain is more sensitive to human serum,
279 even after colonizing the mouse gut (Fig. 3c), therefore being a safer strain for clinical settings than the
280 probiotic EcN.

281 We also checked the non-conjugative plasmid retention in the murine gut by having each strain
282 colonizing germ-free mice carrying the non-conjugative plasmid pMP7605, and quantifying how much of the
283 population retained the plasmid after five days of colonization. EcN lost the plasmid in only 11% of the
284 population, while Kp1012 lost in 51% (Fig. 3d). Remarkably, ARO112 lost the plasmid in more than 99% of
285 cells (Fig. 3d), showing that the recalcitrance of ARO112 to maintaining acquired antibiotic resistances is
286 potentiated in the murine gut.

287 Next, we tested the host reaction to the colonization by each of the three aforementioned strains,
288 by assessing the fecal levels of Lipocalin-2 (Lcn2), as a marker for gut inflammation[54,55]. After 5 days of mono-
289 colonization, fecal levels of Lcn2 in mice colonized with ARO112 were similar to germ-free mice, providing no
290 evidence for ARO112 inducing intestinal inflammation in mono-colonized mice (Fig. 3e). This contrasted with
291 colonization with EcN and, to an even greater extent, with Kp1012, which significantly induced Lcn2 when
292 compared to the germ-free mice levels (Fig. 3e). Since Lcn2 decreases bacterial growth through competition
293 for iron by siderophore sequestration, we then tested how these three strains were able to maintain growth
294 with increasing levels of Lcn2, which is commonly increased in the inflamed intestinal environment. ARO112,
295 EcN, or Kp1012 were grown in rich or minimal media in the absence or in the presence of increasing
296 concentrations of Lcn2. ARO112 showed an overall higher resistance than EcN to increased levels of Lcn2
297 (Extended Data Fig. 2b), suggesting a better ability to survive in an inflamed gut environment.

298 Together, these results indicate that ARO112 could be a safe next-generation probiotic since it has
299 reduced resistance to human serum and low pathogenic potential. Moreover, it has low plasmid retention,
300 as opposed to other *Enterobacteriaceae* strains. Additionally, ARO112's ability to endure higher levels of Lcn2
301 with no inflammatory induction, as opposed to EcN, further highlights how this commensal strain is
302 potentially safer and better suited to compete with invading bacteria in intestinal inflammatory
303 environments.

304

305 **ARO112 promotes a faster recovery from AIEC gut infection in an IBD mouse model**

306 Having shown that ARO112 has less potentially harmful features than an MDR *K. pneumoniae* and
307 the probiotic EcN, and that in previous work we also see that ARO112 is able to partially displace *E. coli*
308 MG1655 from the gut of mono-colonized and antibiotic-treated mice[37], here, we decided to test the potential
309 protective role of ARO112 against AIEC. The pathobiont AIEC is particularly problematic under inflammatory
310 conditions, such as those in IBD patients[56]. Therefore, we reasoned that the low inflammatory potential of
311 ARO112 and its capacity to endure Lcn2 could be beneficial in the IBD context.

312 It was previously shown that a genetic-based murine model for IBD, Nod2$^{-/-}$ mutant mice, is more
313 susceptible to AIEC colonization after antibiotic treatment, similar to IBD patients, as clearance of this
314 pathobiont is slower in the Nod2$^{-/-}$ animals than in WT animals[57]. Additionally, like IBD patients, Nod2$^{-/-}$
315 animals are more prone to gut inflammation increases[58,59]. Therefore, we started by comparing susceptibility
316 of WT and Nod2$^{-/-}$ mice to colonization by AIEC in our animal facility. All mice were treated by oral gavage
317 with a combination of two non-absorbed antibiotics used in clinical settings on IBD patients[60], vancomycin
318 and gentamicin, once daily for three consecutive days[57] (Fig. 4 and Extended Data Fig. 3a). After antibiotic
319 treatment, mice were gavaged with AIEC, and AIEC colonization was followed through selective plating. As
320 observed by others[57], Nod2$^{-/-}$ mice were more susceptible to AIEC colonization in comparison with WT mice,
321 with ~50% of the Nod2$^{-/-}$ mice still being colonized with AIEC after 20 days of infection (Fig. 4b, control
322 animals), while all WT mice had cleared the infection in that same timeframe (Extended Data Fig. 3a, control
323 mice). To test the therapeutic potential of ARO112, one day following AIEC infection, Nod2$^{-/-}$ mice were
324 gavaged with either ARO112 strain or the probiotic EcN strain (Fig. 4a). AIEC decolonization was faster in
325 mice treated with ARO112, with 50% of the animals being AIEC-free at 8 days of infection (7 days of probiotic
326 treatment), compared to mice that received no probiotic treatment (+PBS, control mice), in which 14 days
327 were needed for 50% of the mice to resolve the infection, and 7 out of 15 mice still remained infected at the
328 end of treatment (Fig. 4b,c). Surprisingly, treatment with the probiotic EcN did not help decolonization, but
329 actually resulted in a worse outcome, with all but one tested mice remaining infected with high levels of AIEC
330 for the 20 days of the experiment (Fig. 4b,c). We highlight that EcN failed to colonize the one mouse of this
331 group that displaced AIEC infection and therefore, the displacement observed in this animal is not attributed
332 to the EcN treatment (Extended Data Fig. 3b). When assessing the number of mice that resolve the infection
333 in each condition, it is evident that treatment with EcN promotes a continued infection with AIEC, while the
334 absence of probiotic treatment led to the infection being resolved in half of the population (Fig. 4b,c), thus
335 the outcome obtained with the treatment with ARO112, in which 10 out of 12 mice (>83%) became AIEC-
336 free by the end of the experiment, was more efficient than the control (Fig. 4b). Additionally, we observed
337 that ARO112 is itself cleared from the intestinal microbiota throughout the experiment, after the clearance

338 of AIEC, with a median of 10 days post-AIEC inoculation for the ARO112 loads to drop below detection level
339 in 50% of mice (Extended Data Fig. 3b), having disappeared in 9 out of the 12 mice tested (75%) by the end
340 of the experiment (Extended Data Fig. 3b). The protective effect of ARO112 observed in Nod2$^{-/-}$ mice was not
341 seen in WT mice treated with the same antibiotic regimen, as in these animals AIEC decolonization occurs
342 even without treatment (Extended Data Fig. 3a).

343 We have previously shown that ARO112 could partially displace MG1655 in WT mice with a more
344 severe antibiotic treatment of two weeks of streptomycin in the drinking water[37], which drastically affects
345 the microbiota composition[61] and facilitates *Enterobacteriaceae* colonization that compete for the available
346 carbon sources. In streptomycin-treated animals, ARO112 reduced MG1655 colonization largely by a direct
347 interaction between these 2 species through nutrient competition, as the ARO112-dependent inhibition of
348 MG1655 could be observed with laboratory cultures and in germ-free mono-colonized mice[37]. We tested the
349 effect of ARO112 and EcN on AIEC in streptomycin-treated WT mice where, in contrast to what we had
350 observed with MG1655, neither ARO112 nor EcN were able to displace AIEC (Extended Data Fig. 3c).
351 Moreover, in the absence of a microbiome in mono-colonized mice with AIEC, a limited displacement of AIEC
352 was obtained upon co-colonization with ARO112 (~4 fold; Extended Data Fig. 3d), which was similar to what
353 was observed when co-colonized with other *Enterobacteriaceae* like the MDR clinical isolates Ec1898 and
354 Kp1012 (>4 and ~6 fold, respectively; Extended Data Fig. 3e,f), but lower than the >10 fold seen previously
355 against MG1655[37] or against other Pseudomonadota species like *Vibrio cholerae* (>38; Extended Data Fig.
356 3g). Interestingly, when co-cultured in vitro in static conditions in minimal medium to test for competition
357 for carbon sources, ARO112 also had a minimal effect on AIEC growth as opposed to EcN that seemed to
358 highly reduce AIEC loads (Extended Data Fig. 3h). Together, these results showing that ARO112 weakly
359 inhibits AIEC in vitro, in the absence of other microbiota members (germ-free) or in the presence of low
360 complex microbiota (after streptomycin treatment), indicating that the interaction between these two
361 bacteria is not driven by nutrition competition. Therefore, the mechanisms explaining the displacement of
362 AIEC in the Nod2$^{-/-}$ animals do not seem to rely on a direct ARO112 effect on AIEC colonization and rather
363 indicate the potential involvement of the gut microbiota. Additionally, the above results highlight that
364 ARO112 can have a broad range effect on different Pseudomonadota pathogens, but the mechanism might
365 be different for different competitors.

366

367 **ARO112 treatment promotes microbiota recovery, namely potential butyrate-producing bacteria depleted**
368 **by antibiotic treatment**

369 To further understand the effect of ARO112 on AIEC in the IBD model, we evaluated a possible role
370 of the gut microbiota in this process. We analyzed the microbiota composition of Nod2$^{-/-}$ mice by 16s rRNA

371 gene sequencing before (pre-AB) and after (post-AB) antibiotic treatment, as well as post-AIEC colonization
372 and after 20 days of treatments with PBS, EcN, or ARO112. We observed that mice treated with ARO112
373 showed a significant recovery in richness and a tendency in recovery of diversity, unlike the long-lasting
374 decrease of both metrics in the mice that received no probiotic treatment or EcN, which persisted as low as
375 just after the antibiotic treatment (Fig. 5a,b). This microbiota recovery promoted by the treatment with
376 ARO112 can help explain both the better displacement of AIEC in this group, but also the displacement of
377 ARO112 itself (Extended Data Fig. 3b), as we expect the recovering microbiota to develop colonization
378 resistance.

379 We then analyzed which of the most abundant taxa (37 taxa representing an average of 98%
380 abundance of all taxa) were affected by the antibiotic treatment (Fig. 5c). Out of these 37 taxa, 22 (59%) were
381 depleted by the antibiotics, while 7 (19%) were enriched and 8 (22%) remained unchanged by the end of the
382 experiment. The mice from the control group or treated with EcN were able to recover 14% (3 of 22) of taxa
383 depleted by the antibiotic treatment (Fig. 5c). More taxa recovered in the group treated with ARO112 strain,
384 where mice were able to recover 41% (9 of 22) taxa depleted by the antibiotic treatment (Fig. 5c).

385 A more detailed analysis of the groups of bacteria affected by antibiotic treatment showed that of
386 the 8 taxa of potential butyrate producers[62] depleted by the antibiotics (highlighted in green in Fig. 5c), 4
387 recovered upon 19 days post-treatment with ARO112 (*Dorea*, *Lachnospiraceae*, *Oscillibacter* and
388 *Ruminococcaceae*), while only 1 was recovered in the control (*Lachnospiraceae*) and another with EcN
389 treatment (*Alistipes*) (Fig. 5c).

390 A Principal Coordinate Analysis (PCoA) depicting the Bray-Curtis dissimilarity index with the 37 taxa
391 shows that antibiotic treatment significantly changes the microbiota (pre-AB vs post-AB, Extended Data Fig.
392 4a). In all three groups the microbiota composition remained different from pre-AB at day 20 of the
393 experiment (Extended Data Fig. 4a), however, treatment with ARO112 resulted in samples positioning closer
394 to the pre-AB levels (Extended Data Fig. 4b). Moreover, a subset of the microbiota appears to be recovered
395 by ARO112 treatment, the potential butyrate producers that are strongly depleted by antibiotic treatment
396 (Fig. 5c). Bray-Curtis dissimilarity indices with the 8 taxa for potential butyrate producers depleted by
397 antibiotics (*Alistipes*, *Syntrophococcus*, *Ruminococcus*, *Butyricicoccus*, *Dorea*, *Oscillibacter*, unclassified
398 *Lachnospiraceae*, unclassified *Ruminococcaceae*) show that, even though both the PBS and ARO112
399 treatments resulted in microbiomes with a composition significantly closer to the pre-AB levels (Extended
400 Data Fig. 4c), only the population of samples treated with ARO112 is undistinguishable from pre-AB samples,
401 demonstrating an overall recovery of this group of taxa promoted by ARO112 (Extended Data Fig. 4d).

402 In summary, here we show that in a mouse model susceptible to infection and prone to
403 inflammation, ARO112 promotes recovery of the dysbiotic microbiota by increasing a group of microbiota
404 members potentially involved in butyrate production.

405

406 **Probiotic therapy with ARO112 enhances microbiota production of butyrate and prevents intestinal**
407 **inflammation**

408 As described in the above section, treatment with ARO112 leads to a better recovery of microbiota
409 richness and diversity, including potential butyrate-producing bacteria. Studies have tagged short-chain fatty
410 acids (SCFAs) like butyrate, acetate, and propionate as important metabolites in IBD, with depletion of
411 butyrate-producing gut bacteria by antibiotic treatments being considered a clinical outcome in these
412 patients[16,63]. Moreover, oral administration of butyrate to improve IBD outcomes in patients has been
413 previously proposed[64]. Therefore, our observation that ARO112 treatment promotes potential butyrate
414 producers in the microbiota, possibly leading to an increased and sustained production of butyrate within
415 the microbiota and gut epithelium, instead of the need for continuous exogenous administration, could be
416 very relevant. For that reason, we have assessed SCFA concentrations in fecal samples of mice treated with
417 probiotics or untreated (Fig. 6a). In agreement with our previous results showing the increase of potential
418 butyrate-producing bacteria, 19 days of treatment with ARO112 resulted in a clear increase of fecal levels of
419 butyrate when compared to mice treated with PBS or with EcN (Fig. 6a). An increase in isobutyrate (an isomer
420 of butyrate) and acetate was also observed with the ARO112 treatment in comparison with the control group
421 and EcN-treated mice, although not statistically significant. Propionate levels were significantly higher with
422 ARO112 than with PBS, but similar to the levels in EcN group. On the other hand, succinate showed higher,
423 but not significant, values in mice treated with EcN, when compared to mice treated with PBS or ARO112
424 probiotic (Fig. 6a).Butyrate has been linked to intestinal health, with anti-inflammatory properties[65], while
425 succinate has been touted as an inflammation marker[66] and can accumulate during *Enterobacteriaceae*
426 infections[67].

427 Next, we used Lcn2 to evaluate the intestinal inflammatory response of the Nod2$^{-/-}$ mice infected
428 with AIEC and treated with PBS, ARO112, or EcN. Interestingly, treatment with EcN not only led to persistent
429 infection by AIEC but also resulted in persistently high Lcn2 levels (Fig. 6b), unlike PBS treatment, in which
430 Lcn2 levels varied between animals, having a significant but mostly transient increase at day 5 of infection
431 (Fig. 6b). More importantly, mice treated with ARO112 showed persistently low levels of Lcn2, never
432 significantly varying from the levels prior to antibiotic treatment (Fig. 6b).

433 The reduced Lcn2 levels and increased butyrate observed here upon treatment with ARO112 are in
434 accordance with previous reports on the anti-inflammatory properties of butyrate[65,68]. However, because the

435 preventive effect on inflammation promoted by ARO112 treatment was seen as early as 5 days post-
436 infection, for it to be due to the anti-inflammatory properties of butyrate would require recovery of butyrate
437 producers early in the treatment. Therefore, we analyzed the state of recovery of potential butyrate
438 producers depleted by antibiotics at day 5 of infection (4 days of treatment). Results show that ARO112
439 treatment resulted in a significant recovery of three potential butyrate producers, one of which, unclassified
440 *Lachnospiraceae*, already recovered to levels seen before antibiotic treatment (Fig. 6c). To evaluate if this
441 recovery would translate in higher levels of intestinal butyrate, we also measured butyrate levels at day 5,
442 noticing that butyrate levels in the gut of mice treated with ARO112 already showed higher levels than the
443 other two groups. We reason that this early recovery of butyrate production promoted by ARO112 can
444 explain the prevention of inflammatory episodes at that early stage of treatment.

445 These results show that ARO112 treatment promotes recovery of a subset of microbiota, namely
446 butyrate producers depleted by antibiotics, which through increased production of butyrate prevent
447 inflammation, leading to pathogen clearance and better recovery. Moreover, the possible pro-inflammatory
448 potential of EcN also highlights ARO112 as a safer probiotic in both non-inflammatory and inflammatory host
449 states. The ensemble of these results, namely the displacement of AIEC, the prevention of inflammation, and
450 the recovery of the dysbiotic microbiota and butyrate levels, all obtained upon treatment with ARO112, show
451 a three-pronged therapy targeting the hallmarks of IBD (infection, inflammation, and dysbiosis).

452

453 **Discussion**

454 In this study, we show that the microbiota member of the non-*pneumoniae Klebsiella* complex,
455 *Klebsiella* sp. ARO112 strain, is able to displace infections by the pathobiont AIEC in an IBD mouse model.
456 Remarkably, this displacement was not merely driven by a competitive interaction between ARO112 and
457 AIEC. Instead, ARO112 therapy after antibiotics treatment facilitated microbiota recovery, promoting specific
458 members, like *Lachnospiraceae*, and enhancing butyrate production. This recovery had functional
459 consequences and benefits beyond just AIEC displacement, also preventing increased intestinal inflammation
460 during infection.

461 Other recent studies have added encouraging evidence that non-pneumoniae *Klebsiella* microbiota
462 species and strains contribute significantly to protection against *Enterobacteriaceae* infections,
463 demonstrated in animal models and supported by human studies[37,40,41]. One study pinpointed and validated
464 *K. oxytoca* strains present in children's microbiota with protection against invading *K. pneumoniae*[40] . There,
465 the authors showed that nutrition competition played an important role in protection against *K. pneumoniae*,
466 similarly to what we had already shown in a previous publication where ARO112 protected against *E. coli* and
467 *Salmonella* Typhimurium through nutrient competition[37]. A more recent publication studying human samples

468 identified a series of bacterial sequences matching non-*pneumoniae Klebsiella* species (related to *K.*
469 *michiganensis*, *K. oxytoca*, and ARO112) associated with protection against intestinal pathogens with high
470 risk of bacteremia[41]. These three studies support the protective role of non-*pneumoniae Klebsiella* species
471 against *Enterobacteriaceae* invasion, highlighting the role of nutrient competition in this interaction. In
472 contrast, the results from our present study show that direct effects of ARO112 against *E. coli* is strain-
473 dependent, since ARO112 shows less capacity to displace AIEC and MRE strains, than it had shown to displace
474 MG1655[37] or *V. cholerae* in the absence of other microbiota, which also shows that the ability of ARO112 to
475 displace pathogens is not restricted to *Enterobacteriaceae*. This indicates that nutrition competition and
476 inhibitory mechanisms potentially involved in the interactions between these pairs of bacteria are not
477 relevant under the conditions tested, supporting our proposal that ARO112 displacement of AIEC in the IBD
478 mouse model is mediated by its promotion of microbiota recovery. Displacement based on direct
479 interactions, although likely to be useful in many situations, are case specific as they depend on genomic
480 profiles of the protective-pathogen pair[69,70]. On the other hand, the ability of ARO112 to promote
481 displacement through microbiota recovery has broader applications, potentially being effective against a
482 wider range of pathogenic strains as the exact genomic composition of the pathogen is less relevant.

483 Despite the encouraging support for the role of these protective non-*pneumoniae Klebsiella* in
484 colonization resistance, the fact that these bacteria are also *Enterobacteriaceae* raises concerns for clinical
485 applications. *Enterobacteriaceae* pathogens are the major cause of Hospital infections in Europe[71].
486 Remarkably, genome analysis of ARO112 in comparison with other *Enterobacteriaceae* revealed that ARO112
487 has less predicted pathogenic traits. The low pathogenic potential based on predicted functions was
488 supported by our phenotypic tests for traits associated with nosocomial infections. Our results of phenotypic
489 tests for pathogenic traits show that some phenotypes are context-dependent, highlighting the importance
490 of testing cells cultured in different media and, if possible, cells extracted from colonization experiments,
491 before asserting the safety of a specific strain for therapeutic purposes. Notably, ARO112 demonstrated to
492 have a lower pathogenic potential in comparison with the patient isolate Kp1012, and similar or lower than
493 the probiotic EcN, which expresses several traits that are commonly associated with pathogenesis, as
494 previously reported[35,36].

495 In Hospitals, the biggest concern related to *Enterobacteriaceae* infections is the high prevalence of
496 MDR[72], which result in critical clinical situations due to a lack of available alternative treatments. We showed
497 that ARO112 not only is not MDR but also showed a low capacity for acquiring and retaining resistant
498 plasmids carrying antibiotic resistance. Interestingly, genome analysis of ARO112 revealed no evidence for
499 genes predicted to be involved in conjugation, which is a major mechanism for plasmid acquisition in
500 *Enterobacteriaceae*[73].

501 The link between ARO112's ability to displace AIEC and to promote microbiota recovery is likely tied
502 to its impact on potential butyrate producers, namely on the recovery of members of the *Lachnospiraceae*
503 family and the increase of butyrate levels, which were observed as early as 5 days after infection in ARO112-
504 treated animals. Butyrate is known to be important for gut health due to its role in promoting epithelial
505 metabolism and immune regulation and having anti-inflammatory properties[65,74,75]. Butyrate has also been
506 shown to provide colonization resistance to *Salmonella* infections[76,77] and MDR *Enterobacteriaceae*[78,79] by
507 direct inhibition. Similarly, studies have shown the importance of *Lachnospiraceae* in colonization resistance
508 against multiple pathogens vancomycin-resistant enterococci (VRE)[80], *Clostridium difficile*[81], *Salmonella*
509 Typhimurium[70], and *Listeria monocytogenes*[82]. In a previous study, we observed that the presence of
510 microbiota members from *Lactobacillus* genus could restrict MRE colonization by promoting the expansion
511 of Clostridiales, with an increase in butyrate levels observed in both mice and antibiotic-treated leukemia
512 patients[79]. However, in that study, even though addition of *Lactobacillus* could decrease MRE gut invasion by
513 two orders of magnitude, complete clearance was never obtained. Additionally, cocktails containing
514 *Lactobacillus* are often used as probiotics but can delay natural microbiota compositional recovery in healthy
515 individuals[33]. In contrast, the effect obtained by ARO112 treatment in the IBD mouse model resulted in
516 clearance of the pathobiont AIEC with a success rate of more than 80%, alongside an accelerated microbiota
517 recovery.

518 Other studies also support the notion that many mechanisms of colonization resistance require
519 positive interactions among unrelated microbiota members to promote colonization resistance and
520 pathogen clearance[79,80]. Here, we describe an innovative ARO112 therapeutic effect that goes beyond
521 infection clearance, showing that in an IBD model, ARO112 promotes the recovery of native butyrate
522 producers depleted by antibiotic treatment while preventing inflammatory flares in the process. Therefore,
523 the therapeutic effect of ARO112 is multifactorial, affecting all three main hallmarks of intestinal
524 inflammatory disorders: susceptibility to infection, dysbiosis, and gut inflammation.

525 Currently available probiotics therapies often show low efficacy largely due to common caveats: 1)
526 unable to colonize long enough to actuate, 2) cause delay in natural microbiota recovery and 3) contribute
527 to the increase of antibiotic resistance transfer[33,34,38,83]. However, ARO112 strain does not display any of these
528 caveats in the IBD murine model studied here. ARO112 not only does not delay microbiota recovery, but
529 actually promotes recovery while also having the advantage of being cleared from the gut in the process. This
530 is in striking contrast with what happened with the probiotic EcN, which delayed microbiota recovery,
531 prolonged AIEC colonization and persisted in the gut at high loads, resulting in increased levels of gut
532 inflammation.

533 Having a safe protective microbiota member that can be used to promote a faster recovery of an
534 imbalanced microbiota and displace pathogens or pathobionts, while preventing inflammatory flares in a

535 disease context is of great therapeutic importance. This safe and effective approach opens new avenues for
536 probiotic research and therapeutic development, offering potential solutions for a range of other clinically-
537 relevant disorders. Further exploration of ARO112's protective mechanisms under different contexts will
538 advance our understanding and enable the identification of additional safe therapeutic microbiota members
539 or consortia for clinical use.

540

541 **Acknowledgements**

542 We thank the members of the Bacterial Signalling Laboratory at Instituto Gulbenkian Ciência and
543 Tanja Dapa, and João Xavier for critically reading the manuscript. In particular, we thank Joana Amaro for the
544 help processing samples for genomic sequencing and metabolomics. We also thank Instituto Gulbenkian
545 Ciência's Animal Facility, in particular Joana Bom, and the Genomics Facility, namely João Sobral, for the help
546 provided during this project's execution. The authors would like to thank the Microbiology Service from the
547 Hospital La Fé in Valência (Spain) for isolating and providing the strains Ec1898, Kp834, and Kp1012. I would
548 like to thank Gabriel Nuñez for providing the AIEC strain (LF82), and Roberto Balbontín-Soria for providing
549 the plasmid pMP7605. We would also like to acknowledge Athanasios Typas for the suggestion to test
550 conjugation from a clinical isolate.

551 This work was funded by Fundação para a Ciência e Tecnologia (FCT-Portugal) projects [PTDC/BIA-
552 MIC/6990/2020] and [SFRH/BPD/116806/2016], as well as by Municipality of Oeiras Proof-of-Concept
553 InnOValley 2022 [IOVPoC-2022-21] and a European Commission grant [MSCA-IF-2018-843183]. Additionally,
554 this project was also funded by InfectERA-ERANET- through FCT-Portugal grant (InfectERA/0004/2015) and
555 Acciones complementarias grant [PCIN-2015-094] from the Spanish Ministerio de Economía y Competitividad
556 and the 7th Research framework program from EU, and a grant from the Spanish MICINN [PID2020-
557 120292RB-I00], granted to KBX and CU, respectively. NMR data were acquired at CERMAX, ITQB-NOVA,
558 Oeiras, Portugal with equipment funded by FCT, project AAC 01/SAICT/2016.

559

560 **Author contributions**

561 V.C. and R.A.O conceptualized and designed the research studies with advice and support from K.B.X
562 and C.U.. R.A.O. executed in vitro experiments with support from V.C.. V.C. executed in vivo experiments
563 with AIEC and Kp1012, in SPF wildtype, SPF Nod2$^{-/-}$, and GF wildtype models, with support from R.A.O.. M.B.C.
564 performed in vivo experiments with *V. cholerae* and Ec1898 with support from R.A.O.. M.F.P. performed the
565 NMR. R.A.O. analyzed microbiome sequencing data and V.C. performed the post-analysis. C.U. provided the
566 whole-genome sequencing data for human isolates Kp1012, Kp834, Ec1898. V.C. and R.A.O. analyzed and

interpreted all the data, under the supervision of K.B.X.. V.C. and R.A.O. wrote the first draft of the manuscript with valuable input from K.B.X. and C.U.. All authors critically read and approved the manuscript.

Competing interests

Calouste Gulbenkian Foundation has applied for a patent regarding this work. Vitor Cabral, Rita A. Oliveira, and Karina B. Xavier are the inventors listed on the patent application. Carles Ubeda has participated as a consultant of Vedanta Biosciences and The Zambon Group. There is no direct overlap between the current study and these consulting duties. The rest of the authors do not have any competing interests.

576 **Material and Methods**

577 Bacterial strains, plasmids and culture conditions

578 See Supplementary Table 1 for all species, strains, and plasmids. Unless otherwise specified bacteria
579 were cultured in Lysogenic Broth (LB, here refereed as rich medium) or M9 minimal medium (47.7mM
580 $NaHPO_4$-$7H_2O$, 22mM KH_2PO_4, 8.6mM NaCl, 18.7mM NH_4Cl, 2mM $MgSO_4$, 0.1mM $CaCl_2$, 1mM thiamine)[84]
581 with 0.5% glucose at 37ºC with aeration (shaking at 240 rpm or in static cultures, as specified).

582 Whole genome sequencing

583 *Klebsiella oxytoca* MBC022 was isolated by plating on LB agar the feces of a WT specific pathogen-
584 free (SPF) C57BL/6J mice bred in the animal house facility at Instituto Gulbenkian Ciência. DNA isolation was
585 performed using a previously described protocol[85] from cells in liquid LB at 37 °C with agitation. DNA library
586 and whole genome sequence was obtained at the IGC Genomics facility. Paired-end sequencing of each
587 sample was performed using an Illumina MiSeq Benchtop Sequencer (Illumina), which produced datasets of
588 250 bp read pairs.

589 Ec1898, Kp1012, and Kp834 were isolated from leukemia patients from Hospital La Fe in Valencia
590 (Spain). Genome sequence was obtained as described above in the FISABIO Sequencing facility.

591 All sequences have been deposited in GenBank.

592 Method for phylogenetic tree

593 Phylogenetic tree was obtained using the whole genomes of strains uploaded to the PATRIC BV-BRC
594 browser software (v3.29.20). Parameters used included 100 single-copy genes, using Multiple Alignment
595 using Fast Fourier (MAFFT) Transform alignment program and RAxML Fast Bootstrapping branch support
596 method (v8.2.11).

597 Genome-encoded predicted pathogenic properties and gene products

598 Genomes of all strains were uploaded to the PATRIC BV-BRC[42] browser software (v3.29.20) and
599 analyzed. For each genome, a table containing all predicted pathogenic properties from 9 available
600 databases: 3 for Virulence Factors (Victors, PATRIC_VF, VFDB), 3 for Drug Targets and Transporters
601 (DrugBank, TCDB, TTD), and 3 for antibiotic resistances (PATRIC, CARD, NDARO). The ensemble of these data
602 was downloaded and two merged tables were compiled with the information for all the strains: one
603 displaying the presence or absence of each pathogenic property in each strain, and another including the
604 abundance of each pathogenic property in each strain. Principal Coordinates analyses were performed using
605 either presence/absence of pathogenic properties (Bray-Curtis dissimilarity index for binary/categorical data;
606 one-way PERMANOVA with Bonferroni correction, 999 permutations) or abundance of said pathogenic

607 properties (Euclidean distances for continuous data; one-way PERMANOVA with Bonferroni correction, 999
608 permutations).

609 Genome-encoded gene products relating to clinically-relevant categories (conjugation and conjugal
610 proteins, natural competence, multidrug resistance, transposases, bacteriophages and integrases, CRISPR
611 systems) number of hits were obtained (Supplementary Table 3) and normalized in graphpad Prism software:
612 in each category the highest number was listed as 100%, the lowest as 0%, and the other numbers distributed
613 according to the percentage within this interval.

614 Antibiotic resistance profile

615 Cultures were grown in either rich or minimal medium for 24h at 37ºC with shaking. Cultures were
616 washed once in sterile PBS and adjusted to a final OD_{600} of 0.05 in 150µl/well in the appropriate medium with
617 different concentrations of antibiotics (as specified). These cultures were then grown for 24h in a 96-well
618 plate in a plate shaker, after which OD_{600} measurements were performed in a plate reader Multiskan Sky.
619 Strains were considered resistant if in the presence of antibiotic could reach at least 80% of the growth
620 obtained in the absence of antibiotic. If growth in the presence of antibiotic was more than 40% and less
621 than 80% of the control growth, the strain was considered intermediate for resistance, and sensitive if grown
622 less than 40% of control growth. Resistance or intermediate resistance to one antibiotic of any class is
623 considered resistance or intermediate resistance to that class of antibiotics. Sensitivity to a class of antibiotics
624 means that bacteria were sensitive to all antibiotics tested of that class. A strain was considered multidrug
625 resistant (MDR) if it was non-susceptible (sensitive or intermediate) to at least 1 antimicrobial agent in 3 or
626 more antimicrobial classes, in both tested media, as defined before[17].

Class	Antibiotic	Concentration (µg/ml)
β-lactam	ampicillin	100
	carbenicillin	50
Aminoglycosides	streptomycin	100
	kanamycin	50
	gentamicin	15
	neomycin	200
	apramycin	50
	spectinomycin	50

Chloramphenicol	chloramphenicol	25
Macrolides	erythromycin	125
Rifamycins	rifampicin	20
Tetracyclines	tetracycline	10
Fluoroquinolones	ciprofloxacin	0.5
	trimethoprim	4
Naphthyridone	nalidixic acid	32
Cephalosporins	cefotoxidine	8

627

628 Biofilm formation

629 Biofilm formation assays were performed by adapting a previously published method (Reisner, 2006;
630 O'Toole, 2011). In summary, bacterial cultures were grown for 24h in either rich or minimal media at 37ºC
631 with shacking. The following day, each culture was washed once in sterile PBS, and final OD_{600} adjusted to
632 0.05 in the appropriate medium and 200 μl of culture were dispensed per well in 48-well plates. Plates were
633 centrifuged for 5 min at 4000 rpm at room temperature, after which plates were incubated at 37ºC for 90
634 min for adhesion. After adhesion, supernatants were carefully removed and discarded, wells were washed
635 once with 200 μl of sterile PBS, and 500 μl of sterile fresh appropriate medium were carefully dispensed per
636 well. Plates were incubated at 37ºC for 24h, after which attached biofilms (biomass) was quantified with
637 Crystal Violet (CV). For that supernatants were removed and discarded and well bottoms were carefully
638 washed with 500 μl of sterile PBS. Each well was carefully stained with 0.1% CV solution and plates were
639 incubated at room temperature for 20 min protected from light. After incubation, each well was washed with
640 PBS and plates were incubated open and inverted in a paper towel for 30 min protected from light, to dry.
641 Each well was then de-stained with 200μl of a 33% glacial acetic acid solution and incubated for 15 min at
642 room temperature protected from light. Supernatants were removed from each well into a new plate and
643 read for OD_{580} in a Multiskan Sky plate reader (peak for CV staining), to quantify biofilm biomass.

644 Urease activity

645 Cultures were grown in either rich or minimal medium for 24h at 37ºC with shaking. Cultures were
646 washed once in sterile PBS and adjusted to an OD_{600} of 1, after which each culture was diluted 20x in urea
647 medium (3g/L L-tryptophan, 5 g/L NaCl, 1g/L H_2KO_4P, 1g/L $H_2K_2O_4P$, 20g/L urea, 0,012g/L phenol red) and
648 incubated for 24h at 37ºC with shaking. Urea degradation leads to the medium color to change from
649 yellow/orange to pink/red. 100 μl of each culture were then transferred into a 96-wellplate and measured

650 at OD_{560} in a Multiskan Sky plate reader to quantify urease activity. For urease activity measurement of
651 bacteria extracted from fecal samples of monocolonized mice, cell suspensions of $2.5x10^7$ cells/ml were used,
652 instead of the grown culture.

653 Siderophore production

654 Cultures were grown in either rich or minimal medium for 24h at 37ºC with shaking. Cultures or fecal
655 samples diluted in PBS were centrifuged to recover supernatants. Culture and fecal supernatants were
656 filtered in 0.22 μm filters. Cell-free supernatants (100 μl) were mixed 1:1 (v:v) with Cas-PIPES solution (100
657 μl) (Alexander & Zuberer, 1991; Das & Barooah, 2018) in a 96-well plate and incubated at room temperature
658 for 20 min, after which OD_{630} was measured in Multiskan Sky plate reader to calculate percentage of
659 siderophore production, using sterile media or PBS as reference.

660 $$\%\ siderophores = \frac{(ref - sample) * 100}{ref}$$

661 Resistance to pooled human serum

662 Bacterial susceptibility to human serum was tested as described (Podschun, 1993) with
663 modifications. Bacterial strains were grown in either rich or minimal medium for 24h at 37ºC with shaking,
664 or extracted directly from fecal pellets. Cultures were washed once in sterile PBS and adjusted to $2x10^7$
665 cells/ml, after which 25 μl of cell suspension in PBS were added to 75 μl of pooled human serum solution
666 (P30-2401, PAN-Biotech). Cultures were plated in LB agar plates for CFUs at 0h and after 3h of static
667 incubation at 37ºC, to assess killing, resistance, or proliferation of bacterial cells in the presence of human
668 serum.

669 Lipocalin-2 in vitro growth

670 Cultures were grown in either rich or minimal medium for 24h at 37ºC with shaking. Cultures were
671 washed once in sterile PBS and adjusted to a final OD_{600} of 0.05 in the appropriate medium with different
672 concentrations of Lipocalin-2 protein. Cultures were grown for 24h in a 96-well plate in a plate reader Biotek
673 Synergy H1 with regular OD_{600} measurements. Final OD_{600} obtained were plotted against the concentration
674 of Lipocalin-2 protein used.

675 Plasmid conjugation

676 Cultures were grown in rich medium for 24h at 37ºC with shaking. Cultures were washed once in
677 sterile PBS. Donor (MG1655 RP4, Kgri RP4) and recipient (ARO112, EcN, Kp1012) strains were thoroughly
678 mixed at a 1:1 ratio (total of 10^8 cells), centrifuged for 30 sec at 14,000 rpm and resuspended in 20 μl of PBS.
679 Two drops of 10 μl each were placed on an agar plate, air-dried, and incubated at 37ºC for 24h. After
680 incubation, both drops were removed with a sterile loop and resuspended in 1 ml of sterile PBS. Serial

681 dilutions were performed and plated to count CFUs for recipient strain with (selective plating with plasmid-
682 borne antibiotic resistance) and without (non-selective or selective plating for recipient's antibiotic resistance
683 plating) tested plasmid. Conjugative plasmid (RP4) harbors resistances to tetracycline (10 μg/ml) and
684 kanamycin (50 μg/ml).

685 Plasmid retention

686 Strains harboring tested plasmids (RP4 acquired through conjugation from MG1655 RP4 donor strain;
687 pMP7605 acquired through electroporation; Kanamycin resistance acquired through conjugation from
688 clinical isolate Kp824) were grown in either rich or minimal medium with antibiotics (for plasmid-borne
689 antibiotic resistances; kanamycin (50 μg/ml) and tetracycline (10 μg/ml) for RP4; gentamicin (30 μg/ml) for
690 pMP7605; kanamycin (50 μg/ml) for transfer from clinical isolate) for 24h at 37ºC with shaking. Cultures were
691 washed once in sterile PBS and adjusted to a final OD_{600} of 0.05 in 150 μl in the appropriate medium without
692 antibiotics, and serial dilutions were plated in selective and non-selective LB agar plates, to assess CFUs with
693 (plasmid retention) and without (plasmid loss) antibiotic resistance. Cultures were incubated at 37ºC with
694 shaking for 24h. Every 24h, cultures were diluted 1:100 in fresh appropriate medium and re-incubated. After
695 5 days of passages, serial dilutions of cultures were plated as mentioned before.

696 Animal experimentation

697 All of the mouse experiments performed at Instituto Gulbenkian Ciência (IGC) were approved by the
698 Institutional Ethics Committee and the Portuguese National Entity (Direção Geral de Alimentação e
699 Veterinária; 015190), which complies with European Directive 86/609/EEC of the European Council.

700 C57BL/6J male mice, either WT or $Nod2^{-/-}$, were used at 6–8 weeks of age and were randomly
701 assigned to experimental and control groups. C57BL/6J mice were used for all experiments. None of the
702 animal experiments were performed blinded. Sample size was chosen according to institutional directives
703 and in accordance with the guiding principles underpinning humane use of animals in research. No statistical
704 analyses were performed to predetermine the sample sizes. All of the experiments were performed at least
705 twice, except when stated otherwise.

706 Bacterial isolation from fecal samples

707 WT C57BL/6J germ-free mice were orally gavaged with 100 µL containing ~10^8 CFUs of ARO112, EcN,
708 or Kp1012 strains bearing the non-conjugative plasmid pMP7605. Five days later, fecal pellets were collected
709 for live gut bacteria extraction, as previously described[51] (Ronda, 2019). Briefly, pellets were weighed and
710 500 µL of sterile PBS were added before mechanical disruption with a motorized pellet pestle, after which
711 another 500 µL of sterile PBS were added. Samples were subjected to four iterations of vortex mixing for 15
712 sec, centrifugation at 1,000 rpm for 30 sec at room temperature and recovery of 750 µL of the debris-free

713 cell-containing supernatants into a new tube, replacing that volume with sterile PBS before the next iteration.
714 After recovery of 3 ml per sample, isolated cells were centrifuged at 4,000 g for 5 min at room temperature,
715 discarding the supernatant and resuspending the cells fractions in 1 ml of sterile PBS supplemented with
716 glycerol and cysteine at final concentrations of 20% and 0.1%, respectively. Samples were frozen and stored
717 at -80ºC, to measure phenotypes (urease activity, human serum resistance, plasmid retention) as described
718 above. Fecal supernatants were used to assess fecal Lipocalin-2 levels and siderophores.

719 Nod2$^{-/-}$ and WT SPF mice experiments

720 C57BL/6J Nod2$^{-/-}$ and WT mice bred under specific pathogen-free conditions in the animal house
721 facility at the Instituto Gulbenkian Ciência were kept individually in sterile ISOcages (Tecniplast) at our specific
722 opportunistic pathogen-free facility. Mice were orally gavaged with gentamicin (3 mg/kg/d) and vancomycin
723 (40 mg/kg/d) once daily for three consecutive days (Drouet, 2012). Two days after the last gavage with
724 antibiotics, mice were orally gavaged with 100µL containing ~10^8 CFUs of AIEC strain (LF82-strepR), and the
725 following day were orally gavaged either with 100 µL of PBS (control), or 100 µL containing ~10^8 CFUs of
726 ARO112 or EcN strains. Fecal samples were collected at the timepoints indicated in the corresponding graph
727 and plated in selective medium to assess colonization levels of AIEC. Additionally, fecal samples were also
728 used to measure levels of Lcn2 (Lipocalin-2/NGAL ELISA) and to determine the intestinal microbiota
729 composition and levels of SCFA.

730 C57BL/6J WT mice bred under SPF conditions in the animal house facility at the Instituto Gulbenkian
731 Ciência were kept individually in ventilated cages with high-efficiency particulate air filters in our animal
732 facility. Streptomycin (5 g/l) was maintained ad libitum in the drinking water for 15 days, being replaced every
733 3 days, after which mice were kept in non-supplemented water. Four days after halting streptomycin
734 treatment, AIEC strain (LF82-strepR) was orally gavaged (~10^8 CFUs/mouse in 100 µL). Three days after that,
735 either ARO112 strain or EcN strain were orally gavaged (~10^8 CFUs/mouse in 100 µL). Fecal samples were
736 collected at the timepoints indicated in the corresponding graph and plated in selective medium to assess
737 colonization levels of AIEC.

738 WT gnotobiotic mice colonization clearance experiments

739 C57BL/6J germ-free mice were bred and raised in IGC's Gnotobiology Unit in axenic isolators (La
740 Calhene/ORM) and were later transferred into sterile ISOcages (Tecniplast). Animals were individually
741 housed and orally gavaged with 100 µL containing ~10^8 CFUs of AIEC (LF82-strepR), Kp1012, *V. cholerae*, or
742 Ec1898 strains. The following day, mice were gavaged with 100 µL containing ~10^8 CFUs of either ARO112 or
743 EcN strains, or 100µl of PBS. Fecal samples were collected at the timepoints indicated in the corresponding
744 graphs and plated in selective media to assess colonization levels of AIEC, Kp1012, *V. cholerae*, or EC1898
745 strains.

746 16S rRNA sequencing

747 All fecal samples from SPF mice experiments stored at −80 °C were processed for DNA extraction as
748 previously described[61]. In brief, DNA was extracted using a combination of the QIAamp Fast DNA Stool Mini
749 Kit (Qiagen) according to the manufacturer's instructions, mechanical disruption using a motorized pellet
750 pestle and elution to a final volume of 100 µL in ATE buffer. For each sample, the 16S rRNA gene was amplified
751 using the 515F/806R (V4 regions) primer pairs recommended by the Earth Microbiome Project under the
752 following PCR cycling conditions: 94 °C for 3 min; 35 cycles of 94°C for 60s, 50°C for 60s and 72°C for 105s;
753 and extension at 72°C for 10min[86,87]. After library preparation, 2 × 250 bp sequencing was performed at the
754 IGC Genomics Unit using an Illumina MiSeq Benchtop Sequencer.

755 Fecal microbiota analysis

756 Mothur v.1.32.1 was used to process sequences as previously described[61], with some modifications.
757 Sequences were converted to FASTA format. Sequences that were shorter than 220 bp containing
758 homopolymers of longer than 8 bp or undetermined bases with no exact match with the forward and reverse
759 primers, and barcodes that did not complement each other or that did not align with the appropriate 16S
760 rRNA variable region, were not included in the analysis. A quality score above 30 (range, 0 to 40, where 0
761 represents an ambiguous base) was used to process sequences, which were trimmed using a sliding-window
762 technique over a 50 bp window. Sequences were trimmed from the 3' end until the quality score criterion
763 was met, and were merged after that. Between 20,000 and 50,000 sequences were obtained per sample.
764 16S rRNA gene sequences were aligned using SILVA template reference alignment[88]. ChimeraSlayer[89] was
765 used to remove potential chimeric sequences. Sequences with distance-based similarity of greater than 97%
766 were joined into the same OTU using the average-neighbor algorithm. All of the samples were rarefied to the
767 same number of sequences (10,000) for diversity analyses. Samples below 10,000 reads were removed from
768 the analysis. A Bayesian classifier algorithm with a 60% bootstrap cut-off was used for each sequence[90];
769 sequences were assigned to the genus level where possible or otherwise to the closest genus-level
770 classification. All OTUs were used, and taxa plotted are the result of the merge of OTUs with the same
771 classification, being collapsed to 37 different taxa, with lower represented OTUs/taxa being summed and
772 plotted as "other". Principal Coordinate Analyses were performed using the 37 taxa or a subset of 8 taxa of
773 potential butyrate producers depleted by antibiotics (*Alistipes*, *Syntrophococcus*, *Ruminococcus*,
774 *Butyricicoccus*, *Dorea*, *Oscillibacter*, unclassified *Ruminococcacea*, unclassified *Lachnospiraceae*),
775 representing the Bray-Curtis dissimilarity index (one-way PERMANOVA with Bonferroni correction and 999
776 permutations).

777 Lipocalin-2/NGAL enzyme-linked immunoassay (ELISA)

778 Fecal samples were weighted and resuspended in 1 ml sterile PBS and mechanically homogenized
779 with a motorized pellet pestle. Samples were centrifuged at 4°C for 15 min at 18,000 xg. Supernatants were
780 recovered and filtered in 0.22 μm filters. ELISA for Lipocalin-2/NGAL (Human Lipocalin-2/NGAL DuoSet ELISA)
781 were performed according to manufacture instructions, except for the volumes used, which were adapted
782 for 384-well plates, instead of 96-well plates. The following volumes were used instead: reagent diluent (40
783 μl/well), sample and standards (20 μl/well), Detection Antibody (20 μl/well), Streptavidin-HRP (20 μl/well),
784 Substrate solution (20 μl/well), Stop solution (20 μl/well).

785 SCFA quantification

786 1H-NMR (proton nuclear magnetic resonance) analysis was performed to determine the abundance
787 of SCFA in the fecal samples collected from Nod2$^{-/-}$ mice treated with ARO112 and EcN, or untreated (control),
788 as previously described[91]. Fecal samples (1 to 3 fecal pellets) were diluted in 1mL of PBS and mechanically
789 homogenized. To remove large debris, the samples were pelleted by centrifugation at 18000 g for 15 min at
790 4°C. Supernatants was collected and filtered through a 0.22 mm filter (Milipore), followed by another
791 filtration step with 3 KDa filters (Vivaspin 500) using centrifugation at 15000 xg and 4°C for 3 h (or until 150
792 μL of filtrate was obtained). Filtered samples were stored at −80°C until spectra were acquired. For spectrum
793 acquisition, samples were thawed at room temperature and 150 μL of sample mixed with 60 μL of 350 mM
794 phosphate buffer (pH 7.09 with 2% NaN3, 10 μL of a 0.05% (w/v) 3-(Trimethylsilyl)propionic-2,2,3,3-d4 (TSP-
795 d4, Sigma-Aldrich) solution, and 380 μL of deuterated water - D_2O) (for a total volume of 600 μL). This mixture
796 was transferred to a 5 mm glass NMR tube. All solutions were prepared with D_2O. Samples were homogenized
797 by inversion and the spectra were acquired after pH measurement. Acquisitions were performed on a Bruker
798 NEO 500MHz instrument equipped with QXI H-C/N/P 5 mm probe-head with z-gradients. 1H-NMR spectra
799 were acquired using 1D NOESY pulse sequence with pre-saturation (noesypr1d) under the following
800 conditions: 90 degrees pulse for excitation mixing time 100 ms, acquisition time 4 s, and relaxation delay 1 s.
801 All spectra were acquired with 200 scans at 25°C, with 48,000 data points and 6002 Hz (12 ppm) spectral
802 width (Chenomx acquisition parameters). The recorded 1H-NMR spectra were phase corrected using Bruker
803 TopSpin 4.0.7 and spectra were then analyzed using Chenomx NMR Suite 8.1. Compounds were identified by
804 manually fitting reference peaks to spectra in database Chenomx 500 MHz Version 10. Quantification was
805 based on internal standard peak integration (TSP-d4).

806 Graphical representation and Statistical analyses

807 Phylogenetic tree (Fig. 1a) was done using iTOL (itol.embl.de). Cluster heatmap (Fig. 1b) was done
808 using SRPlot (https://www.bioinformatics.com.cn), using bidirectional clustering, complete cluster method
809 and Euclidean distances. All statistical graphs and statistical analyses presented were done using Graphpad

Prism 8. Principal Coordinate Analyses were obtained with Past4.02 software (https://folk.universitetetioslo.no/ohammer/past) as explained above.

813 **References**

814 1. van der Waaij, D., Berghuis-de Vries, J. M. & Lekkerkerk-v, L. Colonization resistance of the digestive
815 tract in conventional and antibiotic-treated mice. *J. Hyg. (Lond).* **69**, 405–411 (1971).

816 2. Buffie, C. G. & Pamer, E. G. Microbiota-mediated colonization resistance against intestinal
817 pathogens. *Nat. Rev. Immunol.* **13**, 790–801 (2013).

818 3. Kamada, N. *et al.* Regulated virulence controls the ability of a pathogen to compete with the gut
819 microbiota. *Science* **336**, 1325–1329 (2012).

820 4. Caballero-Flores, G., Pickard, J. M. & Núñez, G. Microbiota-mediated colonization resistance:
821 mechanisms and regulation. *Nat. Rev. Microbiol.* **21**, 347–360 (2023).

822 5. Turnbaugh, P. J., Bäckhed, F., Fulton, L. & Gordon, J. I. Diet-Induced Obesity Is Linked to Marked but
823 Reversible Alterations in the Mouse Distal Gut Microbiome. *Cell Host Microbe* **3**, 213–223 (2008).

824 6. Hollister, E. B., Gao, C. & Versalovic, J. Compositional and functional features of the gastrointestinal
825 microbiome and their effects on human health. *Gastroenterology* **146**, 1449–1458 (2014).

826 7. Oliveira, R. A., Cabral, V. & Xavier, K. B. Microbiome–diet interactions drive antibiotic efficacy. *Nat.*
827 *Microbiol.* **6**, 824–825 (2021).

828 8. Sekirov, I. *et al.* Antibiotic-induced perturbations of the intestinal microbiota alter host
829 susceptibility to enteric infection. *Infect. Immun.* **76**, 4726–4736 (2008).

830 9. Fenneman, A. C., Weidner, M., Chen, L. A., Nieuwdorp, M. & Blaser, M. J. Antibiotics in the
831 pathogenesis of diabetes and inflammatory diseases of the gastrointestinal tract. *Nat. Rev.*
832 *Gastroenterol. Hepatol.* **20**, 81–100 (2023).

833 10. Andremont, A., Cervesi, J., Bandinelli, P.-A., Vitry, F. & de Gunzburg, J. Spare and repair the gut
834 microbiota from antibiotic-induced dysbiosis: state-of-the-art. *Drug Discov. Today* **26**, 2159–2163
835 (2021).

836 11. Oliveira, R. A. & Pamer, E. G. Assembling symbiotic bacterial species into live therapeutic consortia
837 that reconstitute microbiome functions. *Cell Host Microbe* **31**, 472–484 (2023).

838 12. Jain, N., Umar, T. P., Fahner, A.-F. & Gibietis, V. Advancing therapeutics for recurrent clostridioides
839 difficile infections: an overview of vowst's FDA approval and implications. *Gut Microbes* **15**,
840 2232137 (2023).

841 13. DeFilipp, Z. *et al.* Drug-Resistant E. coli Bacteremia Transmitted by Fecal Microbiota Transplant. *N.*
842 *Engl. J. Med.* **381**, 2043–2050 (2019).

843 14. Gupta, S., Mullish, B. H. & Allegretti, J. R. Fecal Microbiota Transplantation: The Evolving Risk
844 Landscape. *Am. J. Gastroenterol.* **116**, 647–656 (2021).

845 15. Khan, M. T. *et al.* Synergy and oxygen adaptation for development of next-generation probiotics.
846 *Nature* **620**, 381–385 (2023).

847 16. Santana, P. T., Rosas, S. L. B., Ribeiro, B. E., Marinho, Y. & de Souza, H. S. P. Dysbiosis in
848 Inflammatory Bowel Disease: Pathogenic Role and Potential Therapeutic Targets. *Int. J. Mol. Sci.* **23**,
849 (2022).

850 17. Djukovic, A. *et al.* High Heterogeneity of Multidrug-Resistant Enterobacteriaceae Fecal Levels in
851 Hospitalized Patients Is Partially Driven by Intravenous beta-Lactams. *Antimicrob. Agents*
852 *Chemother.* **64**, (2020).

853 18. Lee, J.-Y. *et al.* High-Fat Diet and Antibiotics Cooperatively Impair Mitochondrial Bioenergetics to
854 Trigger Dysbiosis that Exacerbates Pre-inflammatory Bowel Disease. *Cell Host Microbe* **28**, 273-
855 284.e6 (2020).

856 19. Zou, Y. *et al.* Correlation between antibiotic use in childhood and subsequent inflammatory bowel
857 disease: a systematic review and meta-analysis. *Scand. J. Gastroenterol.* **55**, 301–311 (2020).

858 20. Goethel, A., Croitoru, K. & Philpott, D. J. The interplay between microbes and the immune response
859 in inflammatory bowel disease. *J. Physiol.* **596**, 3869–3882 (2018).

860 21. Albenberg, L. G., Lewis, J. D. & Wu, G. D. Food and the gut microbiota in inflammatory bowel
861 diseases: a critical connection. *Curr. Opin. Gastroenterol.* **28**, 314–320 (2012).

862 22. Frolkis, A. *et al.* Environment and the inflammatory bowel diseases. *Can. J. Gastroenterol.* **27**, e18-24
863 (2013).

864 23. Hviid, A., Svanström, H. & Frisch, M. Antibiotic use and inflammatory bowel diseases in childhood.
865 *Gut* **60**, 49–54 (2011).

866 24. Qiu, P. *et al.* The Gut Microbiota in Inflammatory Bowel Disease. *Front. Cell. Infect. Microbiol.* **12**,
867 733992 (2022).

868 25. Fakhoury, M., Negrulj, R., Mooranian, A. & Al-Salami, H. Inflammatory bowel disease: clinical aspects
869 and treatments. *J. Inflamm. Res.* **7**, 113–120 (2014).

870 26. Irving, P. M., de Lusignan, S., Tang, D., Nijher, M. & Barrett, K. Risk of common infections in people
871 with inflammatory bowel disease in primary care: a population-based cohort study. *BMJ open*
872 *Gastroenterol.* **8**, (2021).

873 27. Pithadia, A. B. & Jain, S. Treatment of inflammatory bowel disease (IBD). *Pharmacol. Rep.* **63**, 629–

874 642 (2011).

875 28. Small, C.-L. N., Reid-Yu, S. A., McPhee, J. B. & Coombes, B. K. Persistent infection with Crohn's
876 disease-associated adherent-invasive Escherichia coli leads to chronic inflammation and intestinal
877 fibrosis. *Nat. Commun.* **4**, 1957 (2013).

878 29. Abraham, B. P. & Quigley, E. M. M. Probiotics in Inflammatory Bowel Disease. *Gastroenterol. Clin.*
879 *North Am.* **46**, 769–782 (2017).

880 30. Schultz, M. Clinical use of E. coli Nissle 1917 in inflammatory bowel disease. *Inflamm. Bowel Dis.* **14**,
881 1012–1018 (2008).

882 31. Matthes, H., Krummenerl, T., Giensch, M., Wolff, C. & Schulze, J. Clinical trial: probiotic treatment of
883 acute distal ulcerative colitis with rectally administered Escherichia coli Nissle 1917 (EcN). *BMC*
884 *Complement. Altern. Med.* **10**, 13 (2010).

885 32. Bischoff, S. C. *et al.* ESPEN guideline on Clinical Nutrition in inflammatory bowel disease. *Clin. Nutr.*
886 **42**, 352–379 (2023).

887 33. Suez, J. *et al.* Post-Antibiotic Gut Mucosal Microbiome Reconstitution Is Impaired by Probiotics and
888 Improved by Autologous FMT. *Cell* **174**, 1406-1423.e16 (2018).

889 34. Montassier, E. *et al.* Probiotics impact the antibiotic resistance gene reservoir along the human GI
890 tract in a person-specific and antibiotic-dependent manner. *Nat. Microbiol.* **6**, 1043–1054 (2021).

891 35. Nougayrède, J.-P. *et al.* A Toxic Friend: Genotoxic and Mutagenic Activity of the Probiotic Strain
892 Escherichia coli Nissle 1917. *mSphere* **6**, e0062421 (2021).

893 36. Olier, M. *et al.* Genotoxicity of Escherichia coli Nissle 1917 strain cannot be dissociated from its
894 probiotic activity. *Gut Microbes* **3**, 501–509 (2012).

895 37. Oliveira, R. A. *et al.* Klebsiella michiganensis transmission enhances resistance to Enterobacteriaceae
896 gut invasion by nutrition competition. *Nat. Microbiol.* (2020) doi:10.1038/s41564-019-0658-4.

897 38. Collado, M. C., Meriluoto, J. & Salminen, S. Role of commercial probiotic strains against human
898 pathogen adhesion to intestinal mucus. *Lett. Appl. Microbiol.* **45**, 454–460 (2007).

899 39. Mirsepasi-Lauridsen, H. C., Vallance, B. A., Krogfelt, K. A. & Petersen, A. M. Escherichia coli
900 Pathobionts Associated with Inflammatory Bowel Disease. *Clin. Microbiol. Rev.* **32**, (2019).

901 40. Osbelt, L. *et al.* Klebsiella oxytoca causes colonization resistance against multidrug-resistant
902 K. pneumoniae in the gut via cooperative carbohydrate competition. *Cell Host Microbe* **29**, 1663-
903 1679.e7 (2021).

904 41. Schluter, J. *et al.* The TaxUMAP atlas: Efficient display of large clinical microbiome data reveals
905 ecological competition in protection against bacteremia. *Cell Host Microbe* **31**, 1126-1139.e6 (2023).

906 42. Olson, R. D. *et al.* Introducing the Bacterial and Viral Bioinformatics Resource Center (BV-BRC): a
907 resource combining PATRIC, IRD and ViPR. *Nucleic Acids Res.* **51**, D678–D689 (2023).

908 43. Lynch, J. P. 3rd, Clark, N. M. & Zhanel, G. G. Escalating antimicrobial resistance among
909 Enterobacteriaceae: focus on carbapenemases. *Expert Opin. Pharmacother.* **22**, 1455–1473 (2021).

910 44. Lerminiaux, N. A. & Cameron, A. D. S. Horizontal transfer of antibiotic resistance genes in clinical
911 environments. *Can. J. Microbiol.* **65**, 34–44 (2019).

912 45. Wang, G., Zhao, G., Chao, X., Xie, L. & Wang, H. The Characteristic of Virulence, Biofilm and
913 Antibiotic Resistance of Klebsiella pneumoniae. *Int. J. Environ. Res. Public Health* **17**, (2020).

914 46. Mobley, H. L. & Hausinger, R. P. Microbial ureases: significance, regulation, and molecular
915 characterization. *Microbiol. Rev.* **53**, 85–108 (1989).

916 47. Nakano, M., Iida, T. & Honda, T. Urease activity of enterohaemorrhagic Escherichia coli depends on
917 a specific one-base substitution in ureD. *Microbiology* **150**, 3483–3489 (2004).

918 48. Clegg, S. & Murphy, C. N. Epidemiology and Virulence of Klebsiella pneumoniae. *Microbiol. Spectr.* **4**,
919 (2016).

920 49. Podschun, R., Sievers, D., Fischer, A. & Ullmann, U. Serotypes, hemagglutinins, siderophore
921 synthesis, and serum resistance of Klebsiella isolates causing human urinary tract infections. *J.*
922 *Infect. Dis.* **168**, 1415–1421 (1993).

923 50. Sonnenborn, U. & Schulze, J. The non-pathogenic Escherichia coli strain Nissle 1917 – features of a
924 versatile probiotic. *Microb. Ecol. Health Dis.* **21**, 122–158 (2009).

925 51. Ronda, C., Chen, S. P., Cabral, V., Yaung, S. J. & Wang, H. H. Metagenomic engineering of the
926 mammalian gut microbiome in situ. *Nat. Methods* **16**, (2019).

927 52. Sheth, R. U., Cabral, V., Chen, S. P. & Wang, H. H. Manipulating Bacterial Communities by in situ
928 Microbiome Engineering. *Trends Genet.* **32**, 189–200 (2016).

929 53. Millan, A. S. *et al.* Positive selection and compensatory adaptation interact to stabilize non-
930 transmissible plasmids. *Nat. Commun.* **5**, 5208 (2014).

931 54. Chassaing, B. *et al.* Fecal lipocalin 2, a sensitive and broadly dynamic non-invasive biomarker for
932 intestinal inflammation. *PLoS One* **7**, e44328 (2012).

933 55. Moschen, A. R., Adolph, T. E., Gerner, R. R., Wieser, V. & Tilg, H. Lipocalin-2: A Master Mediator of

934 Intestinal and Metabolic Inflammation. *Trends Endocrinol. Metab.* **28**, 388–397 (2017).

935 56. Rolhion, N. & Darfeuille-Michaud, A. Adherent-invasive Escherichia coli in inflammatory bowel
936 disease. *Inflamm. Bowel Dis.* **13**, 1277–1283 (2007).

937 57. Drouet, M. *et al.* AIEC colonization and pathogenicity: influence of previous antibiotic treatment and
938 preexisting inflammation. *Inflamm. Bowel Dis.* **18**, 1923–1931 (2012).

939 58. Couturier-Maillard, A. *et al.* NOD2-mediated dysbiosis predisposes mice to transmissible colitis and
940 colorectal cancer. *J. Clin. Invest.* **123**, 700–711 (2013).

941 59. de Souza, P. R. *et al.* Absence of NOD2 receptor predisposes to intestinal inflammation by a
942 deregulation in the immune response in hosts that are unable to control gut dysbiosis.
943 *Immunobiology* **223**, 577–585 (2018).

944 60. Lev-Tzion, R. *et al.* Oral Vancomycin and Gentamicin for Treatment of Very Early Onset Inflammatory
945 Bowel Disease. *Digestion* **95**, 310–313 (2017).

946 61. Thompson, J. A., Oliveira, R. A., Djukovic, A., Ubeda, C. & Xavier, K. B. Manipulation of the Quorum
947 Sensing Signal AI-2 Affects the Antibiotic-Treated Gut Microbiota. *Cell Rep.* **10**, 1861–1871 (2015).

948 62. Vital, M., Karch, A. & Pieper, D. H. Colonic Butyrate-Producing Communities in Humans: an Overview
949 Using Omics Data. *mSystems* **2**, (2017).

950 63. Aden, K. *et al.* Metabolic Functions of Gut Microbes Associate With Efficacy of Tumor Necrosis
951 Factor Antagonists in Patients With Inflammatory Bowel Diseases. *Gastroenterology* **157**, 1279-
952 1292.e11 (2019).

953 64. Di Sabatino, A. *et al.* Efficacy of butyrate in the treatment of mild to moderate Crohn's disease. *Dig.*
954 *Liver Dis. Suppl.* **1**, 31–35 (2007).

955 65. Chen, J. & Vitetta, L. The Role of Butyrate in Attenuating Pathobiont-Induced Hyperinflammation.
956 *Immune Netw.* **20**, e15 (2020).

957 66. Connors, J., Dawe, N. & Van Limbergen, J. The Role of Succinate in the Regulation of Intestinal
958 Inflammation. *Nutrients* **11**, (2018).

959 67. Rosenberg, G. *et al.* Host succinate is an activation signal for Salmonella virulence during
960 intracellular infection. *Science* **371**, 400–405 (2021).

961 68. Byndloss, M. X. *et al.* Microbiota-activated PPAR-gamma signaling inhibits dysbiotic
962 Enterobacteriaceae expansion. *Science* **357**, 570–575 (2017).

963 69. Gül, E. *et al.* Differences in carbon metabolic capacity fuel co-existence and plasmid transfer

964 between Salmonella strains in the mouse gut. *Cell Host Microbe* **31**, 1140-1153.e3 (2023).

965 70. Eberl, C. *et al.* E. coli enhance colonization resistance against Salmonella Typhimurium by
966 competing for galactitol, a context-dependent limiting carbon source. *Cell Host Microbe* **29**, 1680-
967 1692.e7 (2021).

968 71. Friedrich, A. W. Control of hospital acquired infections and antimicrobial resistance in Europe: the
969 way to go. *Wiener Medizinische Wochenschrift* **169**, 25–30 (2019).

970 72. Tacconelli, E. *et al.* Discovery, research, and development of new antibiotics: the WHO priority list of
971 antibiotic-resistant bacteria and tuberculosis. *Lancet. Infect. Dis.* **18**, 318–327 (2018).

972 73. Jones, B. V, Sun, F. & Marchesi, J. R. Comparative metagenomic analysis of plasmid encoded
973 functions in the human gut microbiome. *BMC Genomics* **11**, 46 (2010).

974 74. Furusawa, Y. *et al.* Commensal microbe-derived butyrate induces the differentiation of colonic
975 regulatory T cells. *Nature* **504**, 446–450 (2013).

976 75. Atarashi, K. *et al.* Treg induction by a rationally selected mixture of Clostridia strains from the
977 human microbiota. *Nature* **500**, 232–236 (2013).

978 76. Jacobson, A. *et al.* A Gut Commensal-Produced Metabolite Mediates Colonization Resistance to
979 Salmonella Infection. *Cell Host Microbe* **24**, 296-307.e7 (2018).

980 77. Rivera-Chávez, F. *et al.* Depletion of Butyrate-Producing Clostridia from the Gut Microbiota Drives an
981 Aerobic Luminal Expansion of Salmonella. *Cell Host Microbe* **19**, 443–454 (2016).

982 78. Sorbara, M. T. *et al.* Inhibiting antibiotic-resistant Enterobacteriaceae by microbiota-mediated
983 intracellular acidification. *J. Exp. Med.* **216**, 84–98 (2019).

984 79. Djukovic, A. *et al.* Lactobacillus supports Clostridiales to restrict gut colonization by multidrug-
985 resistant Enterobacteriaceae. *Nat. Commun.* **13**, 5617 (2022).

986 80. Caballero, S. *et al.* Cooperating Commensals Restore Colonization Resistance to Vancomycin-
987 Resistant Enterococcus faecium. *Cell Host Microbe* **21**, 592-602.e4 (2017).

988 81. Buffie, C. G. *et al.* Precision microbiome reconstitution restores bile acid mediated resistance to
989 Clostridium difficile. *Nature* **517**, 205–208 (2015).

990 82. Becattini, S. *et al.* Commensal microbes provide first line defense against Listeria monocytogenes
991 infection. *J. Exp. Med.* **214**, 1973–1989 (2017).

992 83. Merenstein, D. *et al.* Emerging issues in probiotic safety: 2023 perspectives. *Gut Microbes* **15**,
993 2185034 (2023).

994 84. Sambrook, J. *Molecular cloning : a laboratory manual*. (Third edition. Cold Spring Harbor, N.Y. : Cold
995 Spring Harbor Laboratory Press, [2001] ©2001).

996 85. Wilson, K. Preparation of genomic DNA from bacteria. *Curr. Protoc. Mol. Biol.* **Chapter 2**, Unit 2.4
997 (2001).

998 86. Caporaso, J. G. *et al.* Global patterns of 16S rRNA diversity at a depth of millions of sequences per
999 sample. *Proc. Natl. Acad. Sci.* **108**, 4516–4522 (2011).

1000 87. Caporaso, J. G. *et al.* Ultra-high-throughput microbial community analysis on the Illumina HiSeq and
1001 MiSeq platforms. *ISME J.* **6**, 1621–1624 (2012).

1002 88. Pruesse, E. *et al.* SILVA: a comprehensive online resource for quality checked and aligned ribosomal
1003 RNA sequence data compatible with ARB. *Nucleic Acids Res.* **35**, 7188–7196 (2007).

1004 89. Haas, B. J. *et al.* Chimeric 16S rRNA sequence formation and detection in Sanger and 454-
1005 pyrosequenced PCR amplicons. *Genome Res.* **21**, 494–504 (2011).

1006 90. Wang, Q., Garrity, G. M., Tiedje, J. M. & Cole, J. R. Naive Bayesian classifier for rapid assignment of
1007 rRNA sequences into the new bacterial taxonomy. *Appl. Environ. Microbiol.* **73**, 5261–5267 (2007).

1008 91. Barroso-batista, J., Pedro, M. F., Sales-dias, J. & Pinto, C. J. G. Specific eco-evolutionary contexts in
1009 the mouse gut reveal Escherichia coli metabolic versatility.

1010 92. Craig, L., Pique, M. E. & Tainer, J. A. Type IV pilus structure and bacterial pathogenicity. *Nat. Rev.*
1011 *Microbiol.* **2**, 363–378 (2004).

1012 93. Thiennimitr, P. *et al.* Intestinal inflammation allows Salmonella to use ethanolamine to compete
1013 with the microbiota. *Proc. Natl. Acad. Sci. U. S. A.* **108**, 17480–17485 (2011).

1014 94. Palmela, C. *et al.* Adherent-invasive Escherichia coli in inflammatory bowel disease. *Gut* **67**, 574–587
1015 (2018).

1016 95. Buret, A. G., Motta, J.-P., Allain, T., Ferraz, J. & Wallace, J. L. Pathobiont release from dysbiotic gut
1017 microbiota biofilms in intestinal inflammatory diseases: a role for iron? *J. Biomed. Sci.* **26**, 1 (2019).

1018

1019

1020

1021 **Figures**

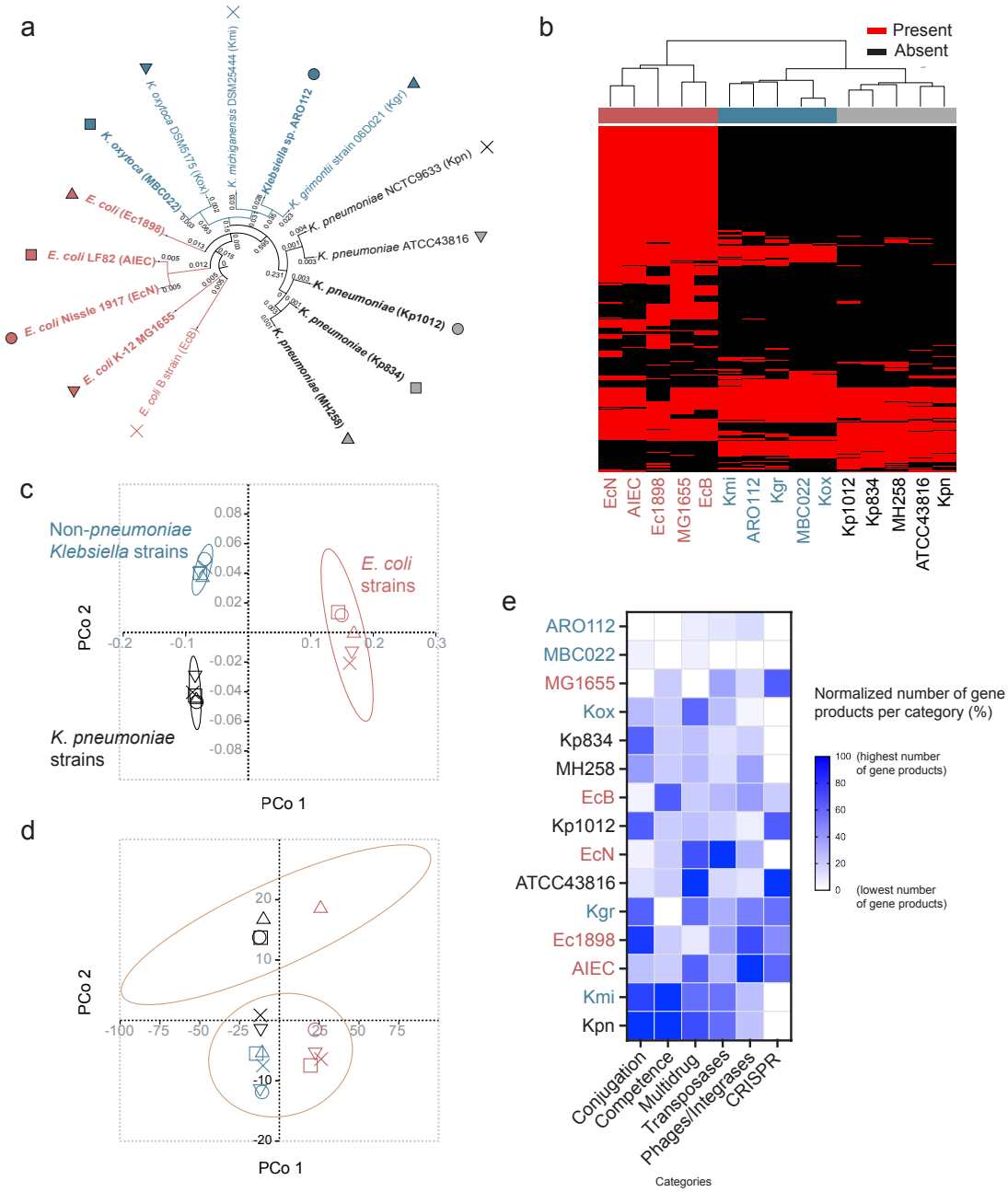

1022

1023 **Fig. 1 | ARO112 genomic comparison with other *Enterobacteriaceae* strains from the *Klebsiella* and**
1024 ***Escherichia* genera for their pathogenic potential. a,** Phylogenetic tree based on whole-genome analysis of
1025 15 strains (5 *E. coli* strains, 5 *K. pneumoniae* strains, and 5 non-*pneumoniae Klebsiella* strains). Strains in bold
1026 were tested experimentally; detailed description of the different the strains in Supplementary Table 1. **b,**
1027 Heatmap, **c,** Principal Coordinate Analysis representing presence/absence of pathogenic properties and **d,**
1028 Principal Coordinate Analysis of the different strains using the abundance of pathogenic properties. **e,**
1029 Normalized quantification of gene products encoding for genes related to clinically-relevant categories

1030 (conjugation and conjugal proteins, natural competence, multidrug resistance, transposases, bacteriophages
1031 and integrases, CRISPR systems). **c-d,** ellipses represent 90% confidence. **e**, highest number per category is
1032 set to 100%, lowest number to 0%, remaining numbers are normalized in between these numbers.

1033

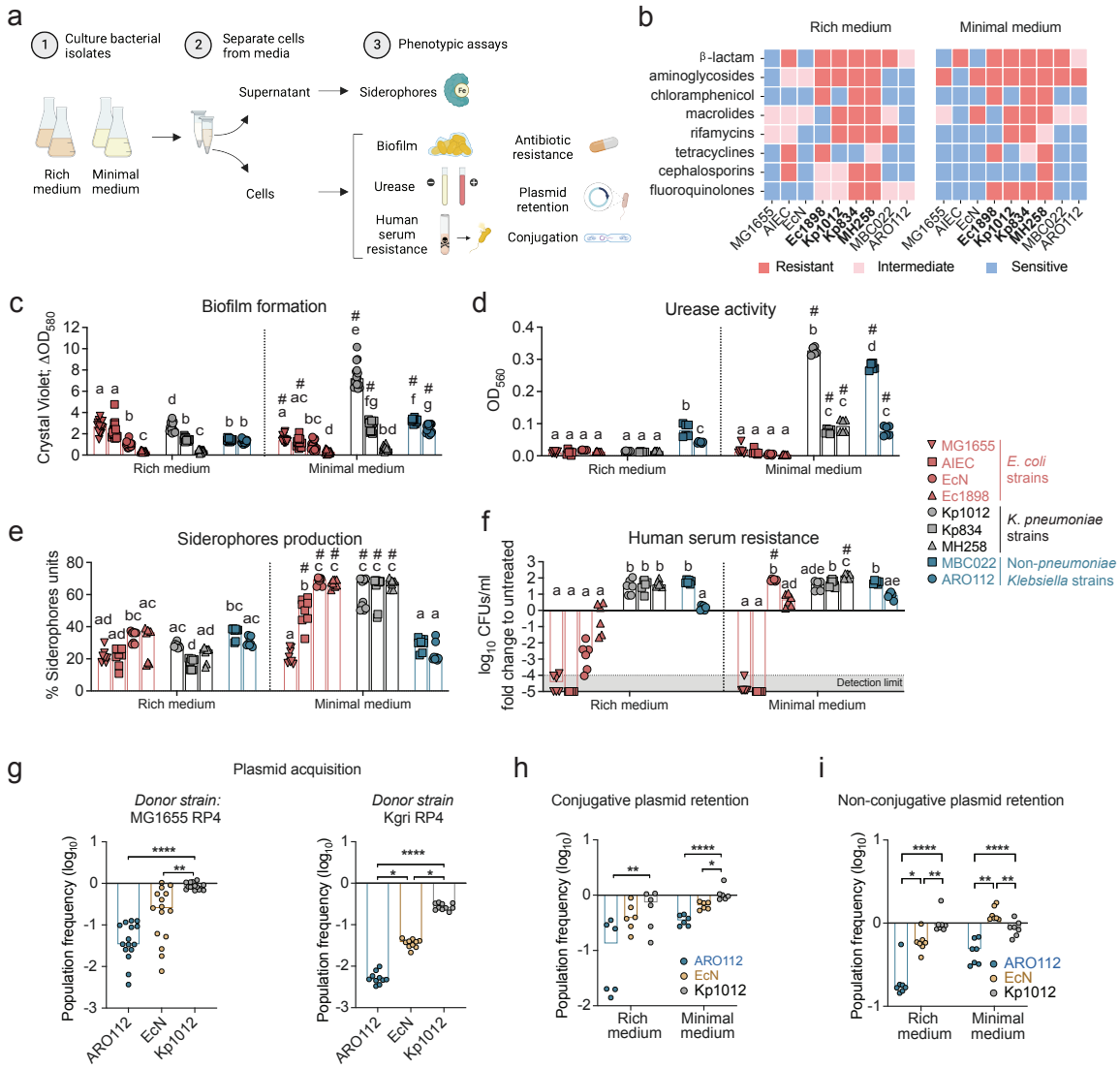

Fig. 2 | Phenotypical evaluation of ARO112 and other *Enterobacteriaceae* strains for nosocomial-related pathogenic factors important for host invasion and colonization. a, Schematic representation of the pipeline used to test bacterial strains for pathogenic traits. A set of 9 strains (4 *E. coli*, 3 *K. pneumoniae*, 2 non-*pneumoniae Klebsiella*) were tested, both in rich and minimal media, for: **b,** antibiotic resistances, MDR *Enterobacteriaceae* strains are represented in bold (resistant to >3 classes of antibiotics); **c,** biofilm formation; **d,** urease activity; **e,** siderophore production; and **f,** capacity to resist killing or inhibition by human serum. Selected strains (ARO112, EcN, and Kp1012) were tested for their capacity to **g**, acquire the conjugative plasmid RP4 from MG1655 donor strain or Kgri donor strain, or **h**, retain the plasmid in rich and minimal media. **i**, The capacity to retain the non-conjugative plasmid pMP7605 in rich and minimal media was also tested. In **c-i**, bars represent median values. **b,** includes data from a total of 6 replicates per group, from 2 independent experiments; **c**, from a total of 15 replicates per group, from 3 independent experiments; **d**, from a total of 6 replicates per group, from 2 independent experiments; **e,** more than 8 replicates per

1048 group, from 3 independent experiments; **f,** from a total of 6 replicates per group, from 2 independent
1049 experiments; **g,** from a total of 15 (from MG1655 RP4) or 10 (From Kgri RP4) replicates per group, from 2-4
1050 independent experiments; **h,** from a total of 6 replicates per group, from 2 independent experiments; **i,** a
1051 total of 7 replicates per group, from 2 independent experiments. In **c-g,** statistical analysis was done using
1052 Kruskal-Wallis' test with Dunn's correction for multiple comparisons. In **e-f,** different letters denote
1053 significant differences among strains within the same medium ($p<0.05$) and # denotes significant differences
1054 between different media for the same strain ($p<0.05$). In **h** and **i**, data were analyzed using Two-way ANOVA
1055 with Sidak's correction for multiple comparisons. * $p<0.05$; ** $p<0.01$; **** $p<0.0001$.

1056

1057

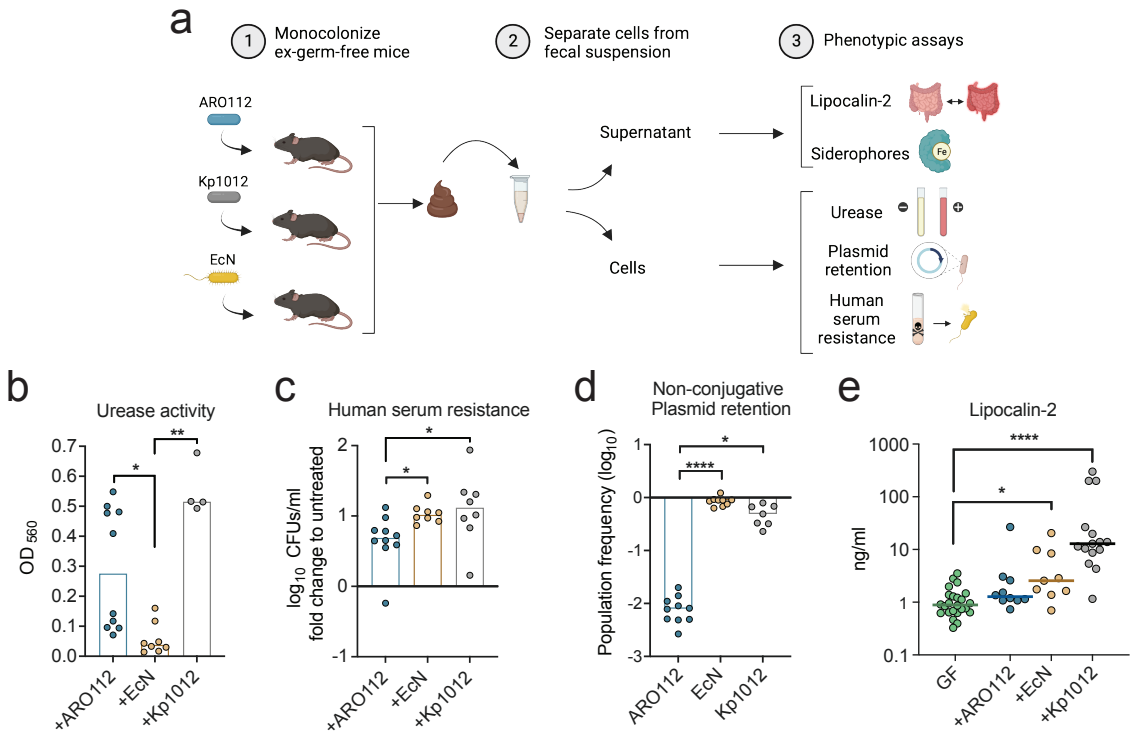

1058

1059 **Fig. 3 | Phenotypic testing of ARO112, EcN, and Kp1012 isolated from fecal samples of mono-**
1060 **colonized mice. a**, Schematic representation of the pipeline used to test bacterial strains for pathogenic traits
1061 after gut colonization. Germ-free (GF) mice were mono-colonized with each of selected strains (ARO112, EcN,
1062 Kp1012) for five days, after which bacteria were isolated from the fecal samples and tested for **b,** urease
1063 activity and **c,** resistance to human serum. **d,** Bacteria were also evaluated for plasmid retention upon
1064 intestinal colonization. **e,** Fecal supernatants were evaluated for Lipocalin-2/NGAL levels, as a marker for
1065 intestinal inflammation. In **b**-**e**, data were analyzed using Kruskal-Wallis' test with Dunn's correction for
1066 multiple comparisons (* $p<0.05$; ** $p<0.01$; **** $p<0.0001$). Urease activity and human serum resistance
1067 from gut isolated bacteria were tested in a total of 10 (ARO112), 8 (EcN), or 4-7 (Kp1012) replicates, from at
1068 least 2-3 independent experiments. Lcn2 was tested in germ-free animals before colonization (GF, N= 24),
1069 and after colonization with ARO112 (N=10), EcN (N=9), or Kp1012 (N=15), from at least 3 independent
1070 experiments. Non-conjugative plasmid retention in gut-isolated bacteria was tested in a total of 10 (ARO112),
1071 9 (EcN), or 7 (Kp1012) replicates, from at least 3 independent experiments. In **b**-**e**, bars and lines represent
1072 median values.

1073

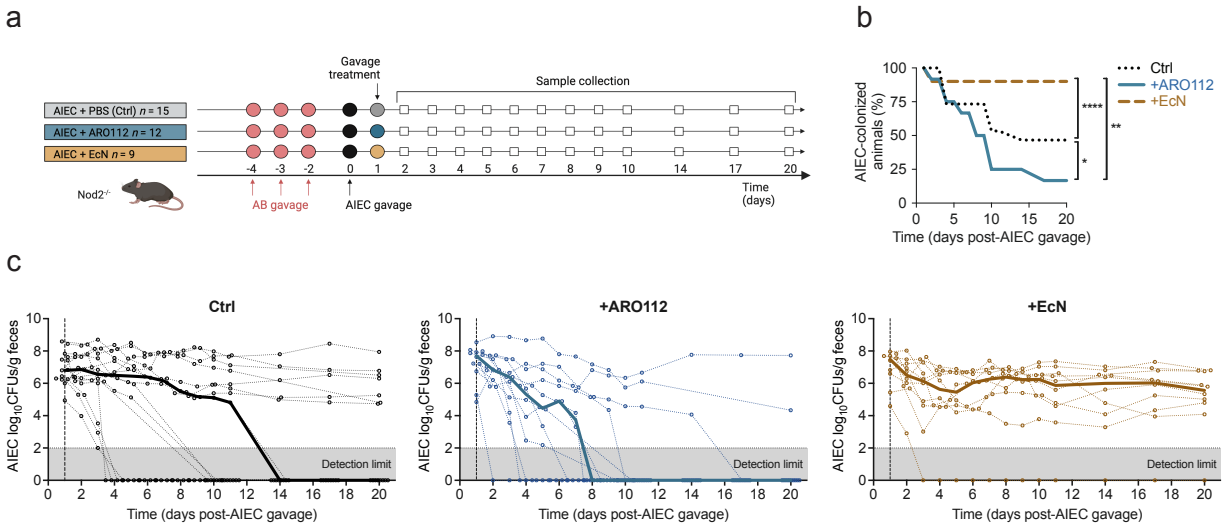

Fig. 4 | Evaluation of therapeutical potential capacities of ARO112 and EcN against AIEC colonization in an IBD mouse model previously treated with antibiotics. a, Experimental setup of IBD mouse model Nod2$^{-/-}$ mice treated with antibiotics, followed by AIEC infection and treated with ARO112, EcN or PBS (Ctrl). **b,** Percentage of mice colonized with AIEC in the different groups throughout the experiment. **c,** AIEC loads during the experiment. Thin lines represent AIEC loads in individual mice over time, while thick lines represent median values for each treatment over time. In **b** and **c**, data were analyzed using Two-way ANOVA with Tukey's correction for multiple comparisons (* $p<0.05$; ** $p<0.01$; **** $p<0.0001$). AIEC fecal loads and colonization were tested in a total of 15 (Ctrl), 12 (+ARO112), or 10 (+EcN) animals, from 2-3 independent experiments.

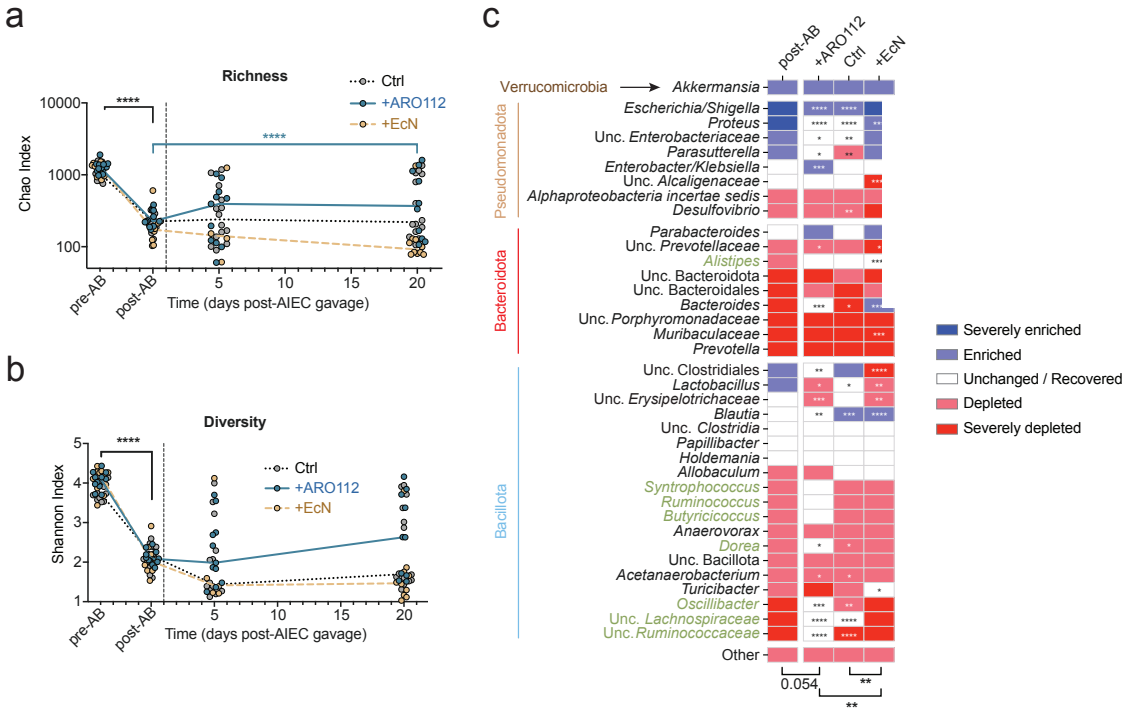

Fig. 5 | Intestinal microbiota composition resultant from treatment with probiotic strains (ARO112, EcN) or lack thereof (Ctrl). a, Richness and **b,** diversity of gut microbiota in fecal samples collected before (pre-AB, day -4), or after (post-AB, day 0) antibiotic treatment and 5 and 20 days after AIEC infections of mice untreated (Ctrl) or treated with ARO112 or EcN. In **a** and **b**, lines represent median values for each treatment over time. **c,** Changes in the relative abundances of most prevalent taxa at day 20 after AIEC infection in comparison with the levels before antibiotics (day -4). In **a**-**c**, data were analyzed using Two-way ANOVA with Dunnett's correction for multiple comparisons (* $p<0.1$; ** $p<0.01$; *** $p<0.001$; **** $p<0.0001$). Fecal microbiota composition analyses were performed in a total of 14 (Ctrl), 10 (+ARO112), or 4-10 (+EcN) samples, from 2-4 independent experiments.

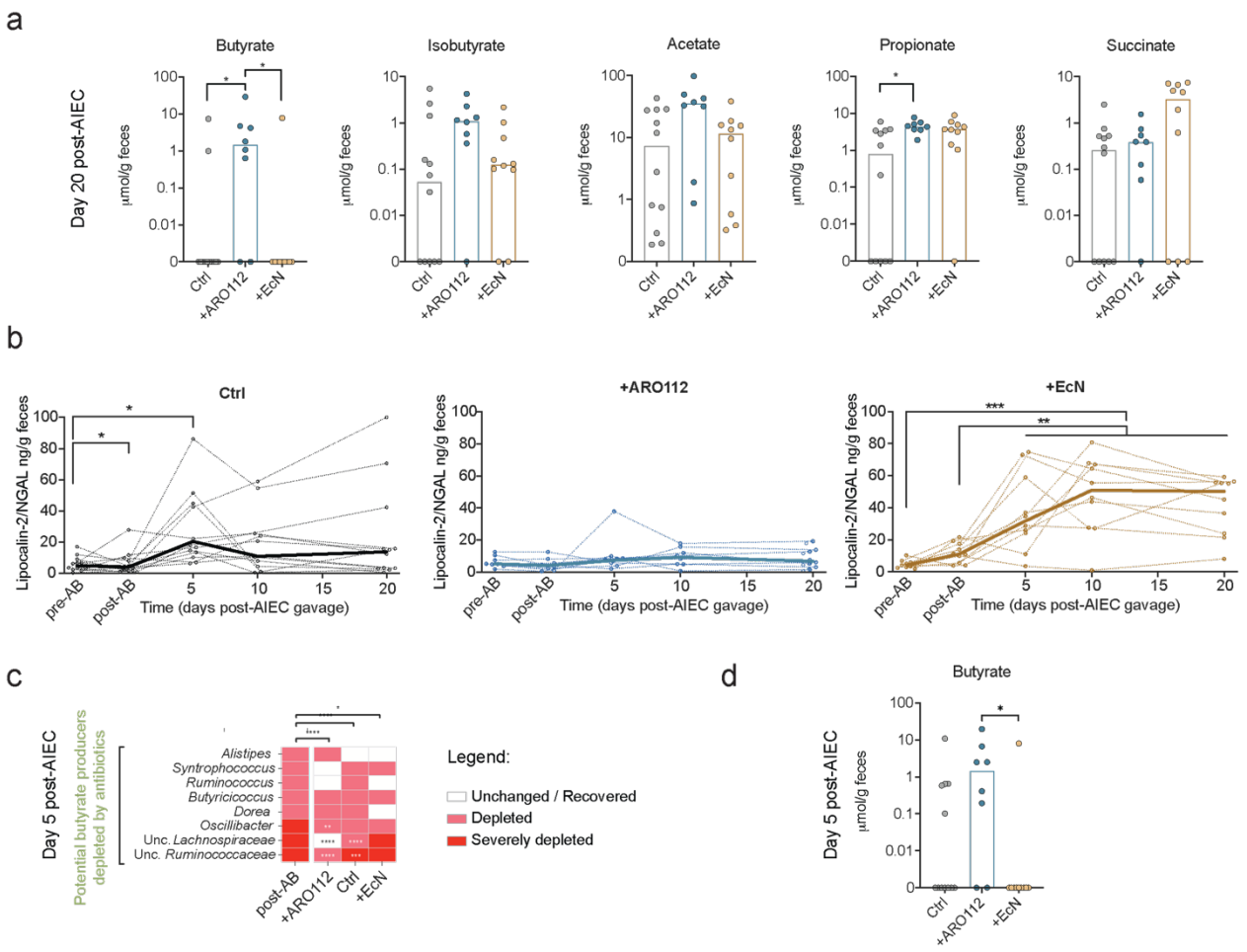

Fig. 6 | SCFA levels and intestinal inflammation profiles of mice upon different probiotic treatments (ARO112, EcN) or lack thereof (Ctrl). a, Metabolomic profile of butyrate, isobutyrate, acetate, propionate, and succinate in fecal samples of IBD mouse model Nod2$^{-/-}$ mice not treated (Ctrl) or treated with probiotics ARO112 (+ARO112) or EcN (+EcN), at the end of the experiment. **b,** Intestinal inflammation was measured via Lcn2 proxy in fecal supernatants, throughout the experiment. Thin lines represent Lcn2 levels in individual mice overtime, while thick lines represent median values for each treatment overtime. **c,** Changes in relative abundances of potential butyrate producers at day 5 after AIEC infection that were depleted by antibiotics, but recovered during experiment. **d,** Metabolomic profile of butyrate in fecal samples of IBD mouse model Nod2$^{-/-}$ mice not treated (Ctrl) or treated with probiotics ARO112 (+ARO112) or EcN (+EcN), at day 5 post-infection (day 4 of treatment). In **a** and **d**, bars represent median values and data were analyzed using Kruskal-Wallis test with Dunn's correction for multiple comparisons. In **b**, data were analyzed using Two-way ANOVA with Tukey's correction for multiple comparisons (* $p<0.05$; ** $p<0.01$; *** $p<0.001$; **** $p<0.0001$). Metabolomics and Lcn2 were tested in 12 (Ctrl), 8 (+ARO112) and 10 (+EcN) samples. In **c**, different colors display $\log_2$ fold changes to pre-AB levels of each mouse – severely depleted (<-5), depleted (<-1), unchanged or recovered (-1 to 1), enriched (>1) and severely enriched (>5), and data were analyzed using Two-way ANOVA with Dunnett's correction for multiple comparisons (* $p<0.1$; ** $p<0.01$; *** $p<0.001$; ****

1113 $p<0.0001$). Fecal microbiota composition analyses were performed in a total of 14 (Ctrl), 10 (+ARO112), or 4-
1114 10 (+EcN) samples, from 2-4 independent experiments.

1115

1116

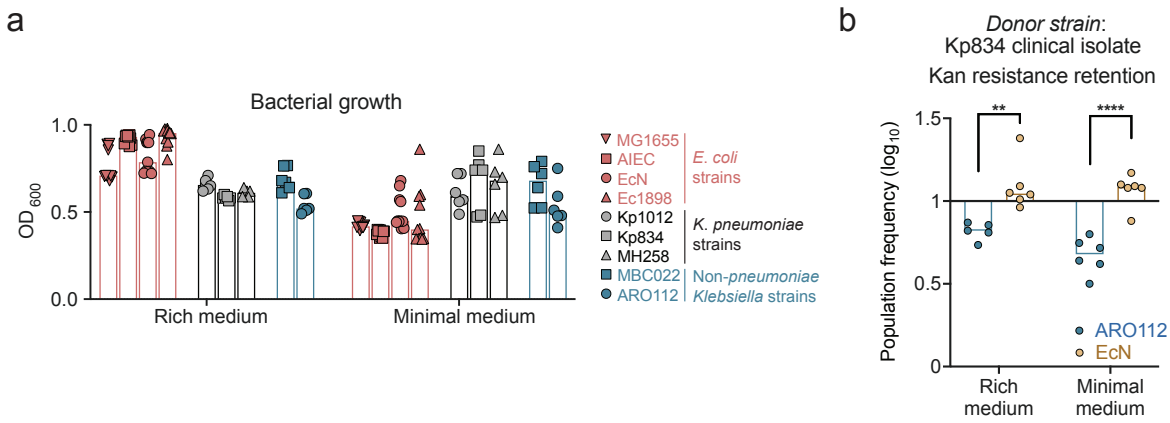

1117

1118 **Extended Data Fig. 1 | Comparison and correlations of phenotypically tested virulence traits. a,**
1119 Bacterial growth in rich and minimal media. **b,** ARO112 and EcN were tested for their capacity to retain a
1120 natural antibiotic-resistant plasmid acquired by conjugation from the clinical isolate Kp834. In **a** and **b**, bars
1121 represent median values. In **b**, data were analyzed using Two-way ANOVA test with Sidak's correction for
1122 multiple comparisons (**p<0.01; **** p<0.0001). Growth was tested in 6-11 replicates, from 2 independent
1123 experiments. Natural conjugative plasmid retention was tested in a total of 5 replicates per group, from 2
1124 independent experiments.

1125

1126

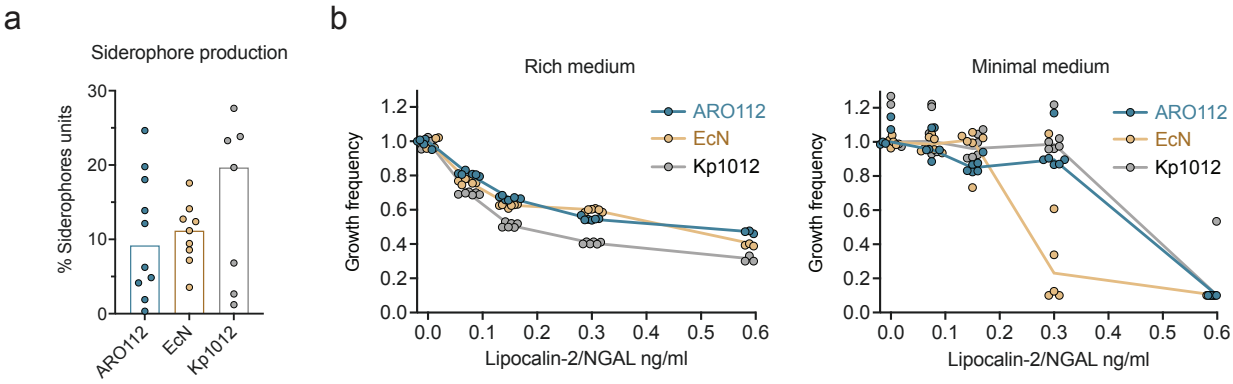

1127

1128 **Extended Data Fig. 2 | Siderophore production in mono-colonized mice and resistance to Lcn2. a,**
1129 Siderophores were measured in fecal supernatants collected from mice mono-colonized with each of
1130 selected strains (ARO112, EcN, Kp1012) for 5 days. Bars represent median values. **b**, Selected strains
1131 (ARO112, EcN, Kp1012) were tested for their capacity to grow in the presence of increased concentrations of
1132 Lcn2 in rich or minimal media. In **a**, siderophore production in fecal samples was tested in a total of 10
1133 (ARO112), 9 (EcN), or 7 (Kp1012) samples, from at least 3 independent experiments. In **b**, Lcn2 resistance
1134 was tested in a total of 6 replicates, from 2 independent experiments, and data were analyzed using Two-
1135 way ANOVA with Tukey's correction for multiple comparisons (* $p<0.05$; *** $p<0.001$; **** $p<0.0001$).

1136

1137

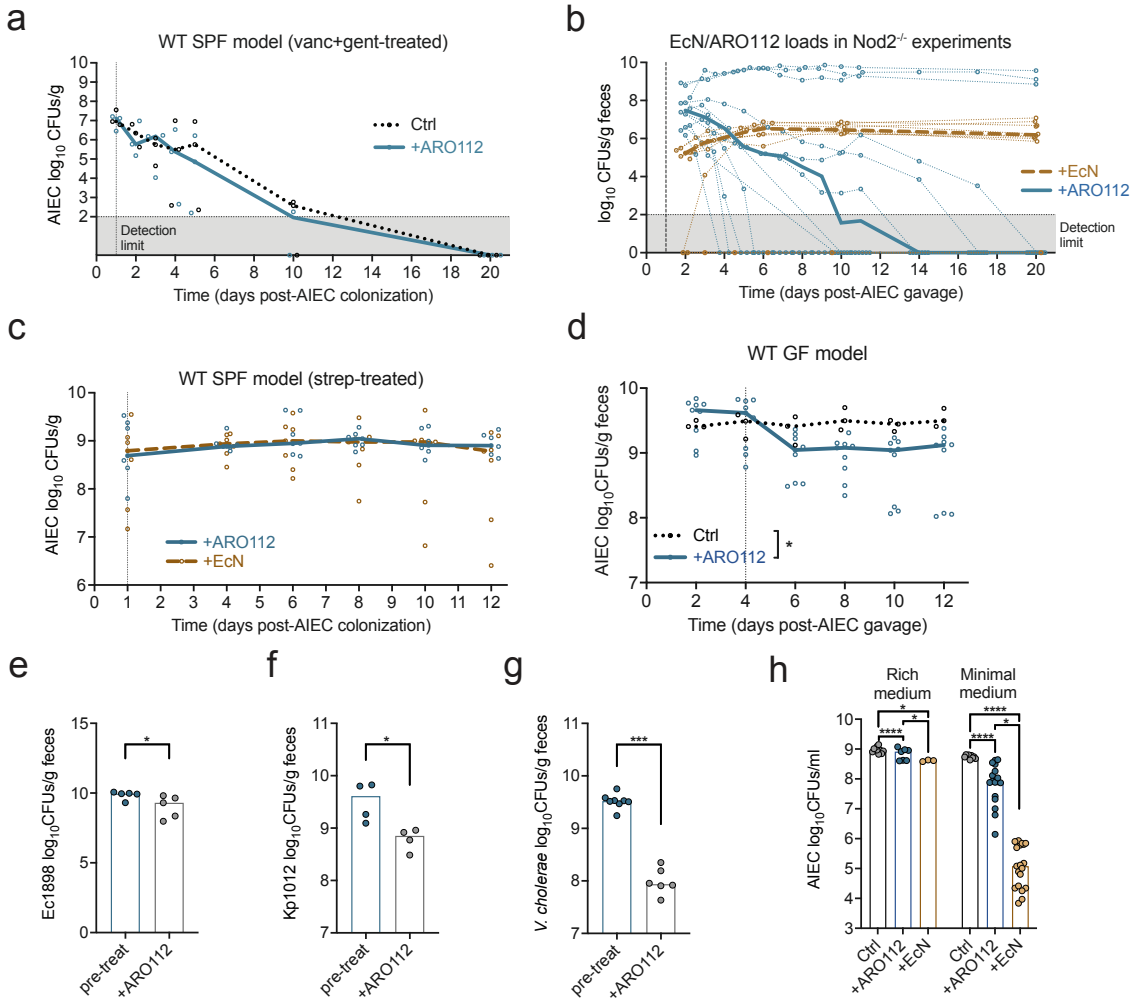

Extended Data Fig. 3 | Probiotic colonization and evaluation of protective capacities of ARO112 and EcN against different invading bacteria in different mouse models. a, Loads of AIEC in fecal samples of WT mice treated with vancomycin and gentamicin and treated with PBS (Ctrl) or ARO112 probiotic (+ARO112). **b,** data from experiment shown in Fig. 4, where **b,** shows the loads of ARO112 or EcN in fecal samples. **c,** Loads of AIEC in fecal samples of WT mice treated with streptomycin and treated with ARO112 (+ARO112) or EcN (+EcN) probiotics. **d,** Loads of AIEC in germ-free WT mice treated with PBS (Ctrl) or ARO112 probiotic (+ARO112). Loads of **e,** Ec1898, **f,** Kp1012**,** and **g,** *V. cholerae* after 4 days of mono-colonization (pre-treat) or after 8 days of treatment with ARO112 (+ARO112), in germ-free WT mice. **h,** Loads of AIEC after 24h of growth without or with ARO112 or EcN, in rich or minimal media. AIEC loads in WT SPF models were tested in 3 replicates per group (**a**) or 7 replicates per group (**c**), from 1 or 2 independent experiments, respectively. Probiotic loads were tested in 12 (+ARO112) or 10 (+EcN) replicates from 2-3 independent experiments (**b**). AIEC loads in WT GF model were tested in 3 (Ctrl) and 9 (+ARO112) replicates in 1-2 independent experiments, and data were analyzed using two-way ANOVA with Sidak's multiple comparison correction (* $p<0.05$) (**d**). Ec1898 loads were assessed in 5 replicates from 2 independent experiments (**e**). Kp1012 loads were assessed in 8 replicates from 2 independent experiments (**f**). *V. cholerae* loads were assessed from 6

1154 replicates from 2 independent experiments (**g**). In vitro growths were tested in 10 (Ctrl), 7 (+ARO112), or 3
1155 (+EcN) replicates in minimal medium, and 9 (Ctrl), 19 (+ARO112), or 19 (+EcN) replicates in rich medium, from
1156 1-4 independent experiments (**h**), and two-way ANOVA was tested with Tukey's multiple comparison
1157 correction (* $p<0.05$; **** $p<0.0001$). In f-h, data were analyzed using Mann-Whitney tests (* $p<0.05$; ***
1158 $p<0.001$). In **b**, thin lines represent ARO112 and EcN loads in individual mice over time, while in **a**, **b**, **d**, **e**,
1159 thick lines and bars represent median values.

1160

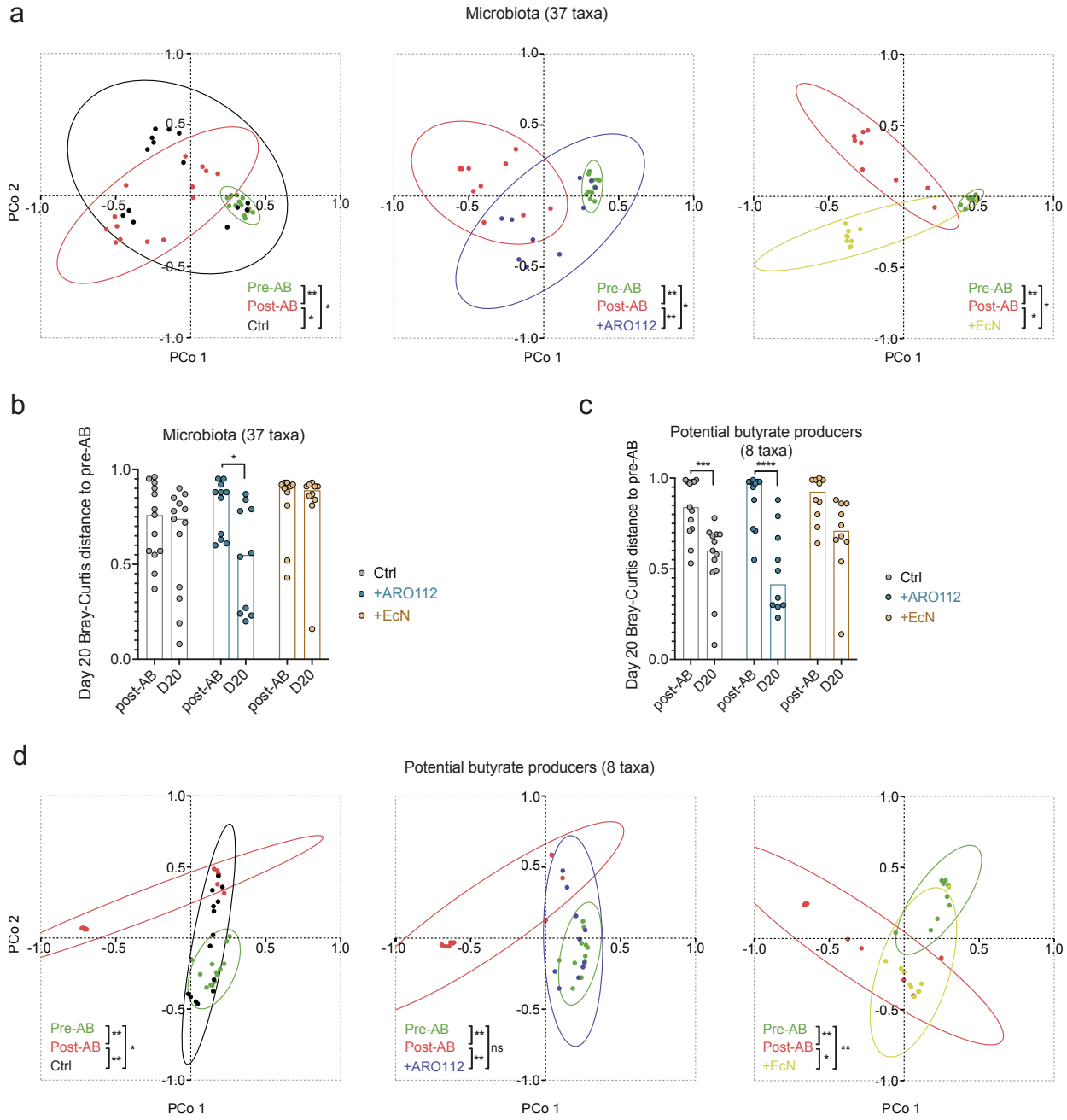

Extended Data Fig. 4 | Comparison between treatments of different microbiota-related parameters in experiment in Nod2$^{-/-}$ mice after 19 days of treatment. a, Principal Coordinate Analysis of Bray-Curtis dissimilarity index displaying clustering of samples before antibiotic treatment (pre-AB), after antibiotic treatment (post-AB), and after treatment (day 20 of experiment) with PBS (Ctrl; 14 samples) or probiotics (+ARO112 or +EcN; 10 samples per group), using microbiota composition (37 taxa). **b,** Analysis of the Bray-Curtis dissimilarity distances, obtained comparing the samples of each mouse pre-AB, to their position post-AB or post-treatment (day 20). **c,** Analysis of the Bray-Curtis dissimilarity distances, obtained comparing the samples of each mouse pre-AB, to their position post-AB or post-treatment (day 20). **d,**

1171 Principal Coordinate Analysis of Bray-Curtis dissimilarity index displaying clustering of samples before
1172 antibiotic treatment (pre-AB), after antibiotic treatment (post-AB), and after treatment (day 5 of experiment)
1173 with PBS (Ctrl; 14 samples) or probiotics (+ARO112 or +EcN; 10 samples per group), for the 8 taxa of potential
1174 butyrate producers depleted by antibiotics (*Alistipes*, *Syntrophococcus*, *Ruminococcus*, *Butyricicoccus*, *Dorea*,
1175 *Oscillibacter*, unclassified *Ruminococcacea*, unclassified *Lachnospiraceae*). Ellipses in **a** and **d** represent 90%
1176 confidence intervals. One-way PERMANOVA with 999 permutations were performed with Bonferroni
1177 corrections (**a** and **d**) and two-way ANOVA were tested with Sidak's correction for multiple comparisons (**b**
1178 and **c**) (* $p<0.05$; ** $p<0.01$; *** $p<0.001$; **** $p<0.0001$).

1179

1180

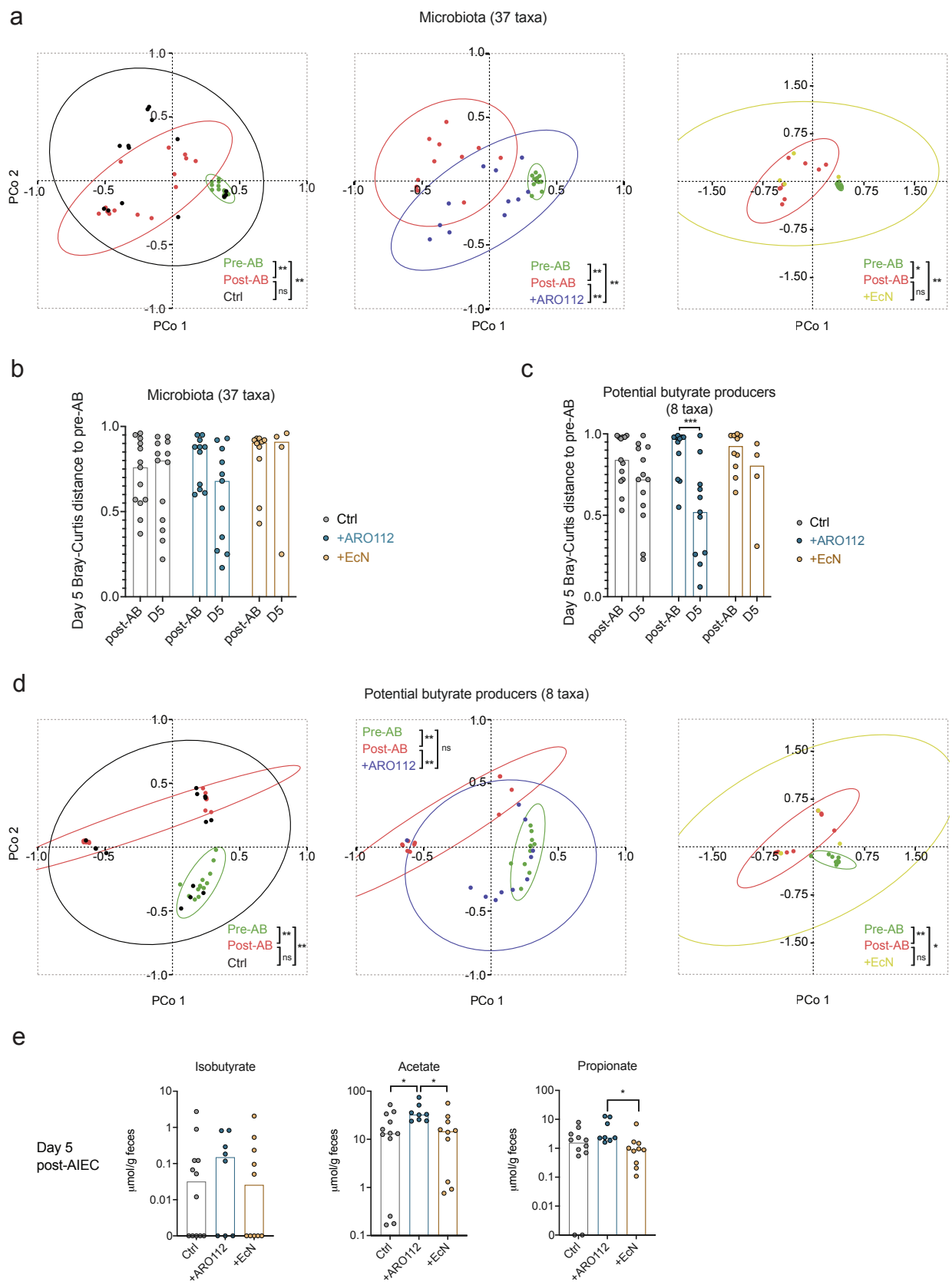

Extended Data Fig. 5 | Comparison between treatments of different microbiota-related parameters in experiment in Nod2$^{-/-}$ mice after 4 days of treatment. a, Principal Coordinate Analysis of Bray-Curtis dissimilarity index displaying clustering of samples before antibiotic treatment (pre-AB), after antibiotic

1185 treatment (post-AB), and after treatment (day 20 of experiment) with PBS (Ctrl; 14 samples) or probiotics
1186 +ARO112 (11 samples) or +EcN (4 samples), using microbiota composition (37 taxa). **b,** Analysis of the Bray-
1187 Curtis dissimilarity distances, obtained comparing the samples of each mouse pre-AB, to their position post-
1188 AB or post-treatment (day 5). **c,** Analysis of the Bray-Curtis dissimilarity distances, obtained comparing the
1189 samples of each mouse pre-AB, to their position post-AB or post-treatment (day 5). **d,** Principal Coordinate
1190 Analysis of Bray-Curtis dissimilarity index displaying clustering of samples before antibiotic treatment (pre-
1191 AB), after antibiotic treatment (post-AB), and after treatment (day 5 of experiment) with PBS or probiotics
1192 (+ARO112 or +EcN), for the 8 taxa of potential butyrate producers depleted by antibiotics (*Alistipes*,
1193 *Syntrophococcus*, *Ruminococcus*, *Butyricicoccus*, *Dorea*, *Oscillibacter*, unclassified *Ruminococcacea*,
1194 unclassified *Lachnospiraceae*). Ellipses in **a** and **d** represent 90% confidence intervals. One-way PERMANOVA
1195 with 999 permutations were performed with Bonferroni corrections (**a** and **d**) and two-way ANOVA were
1196 tested with Sidak's correction for multiple comparisons (**b** and **c**) (* $p<0.05$; ** $p<0.01$; *** $p<0.001$).

1197

1198 **Supplementary Information**

1199 We analyzed the pathogenic properties that are ubiquitous (present in all 5 strains) or non-ubiquitous
1200 (not present in all 5 strains) of each group (Supplementary Table 2). In the non-*pneumoniae Klebsiella* (npK)
1201 strains, there are 64 absent properties when compared to *K. pneumoniae* (Kp) strains, indicating an overall
1202 lower pathogenic potential predicted for the npK group. The difference in absent predicted pathogenic
1203 properties of the npK strains was even higher when compared with *E. coli* (Ec) strains (403), which mainly
1204 included genes encoding for transporters, membrane proteins, and genes potentially conferring resistance
1205 to antibiotics (Fig. 1b, Supplementary Fig. 1, Supplementary Table 2). There are other properties absent in
1206 the npK strains, but present in the Ec strains that are notable, such as genes related to lipopolysaccharide
1207 (LPS) biosynthesis and assembly, flagellum, type IV pilus, toxins, ethanolamine utilization, and hemolysin; all
1208 of which having been associated with virulence and pathogenesis (Supplementary Table 2)[92–95].

1209 We investigated the gene products and predicted genome-encoded pathogenic traits in common
1210 within each clade, i.e., shared by all 5 strains tested per clade, similarly to the aforementioned analysis for
1211 pathogenic properties. A comparison between gene products, which consider the whole genome
1212 (Supplementary Table 3), and the predicted genome-encoded pathogenic properties (Supplementary Table
1213 2), shows that the three clades share a higher percentage of predicted pathogenic traits (47.36%) than gene
1214 products (14.23%; Extended Data Fig. 1a).

1215

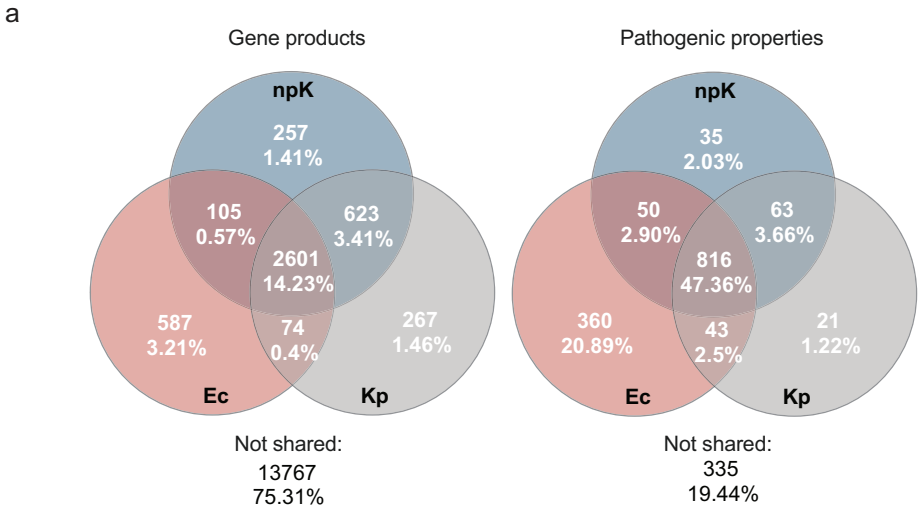

1216

1217 **Supplementary Data Fig. 1 | Comparison between gene products and predicted pathogenic properties.**
1218 Genome analyses were performed in PATRIC BV-BRC software, from where the number of hits for the
1219 different virulence factors databases were obtained. **a,** Venn diagrams of total gene products, shared by
1220 every member of each clade. **b,** Venn diagram of virulence properties' hits shared by every member of each
1221 clade.

Fig. 1

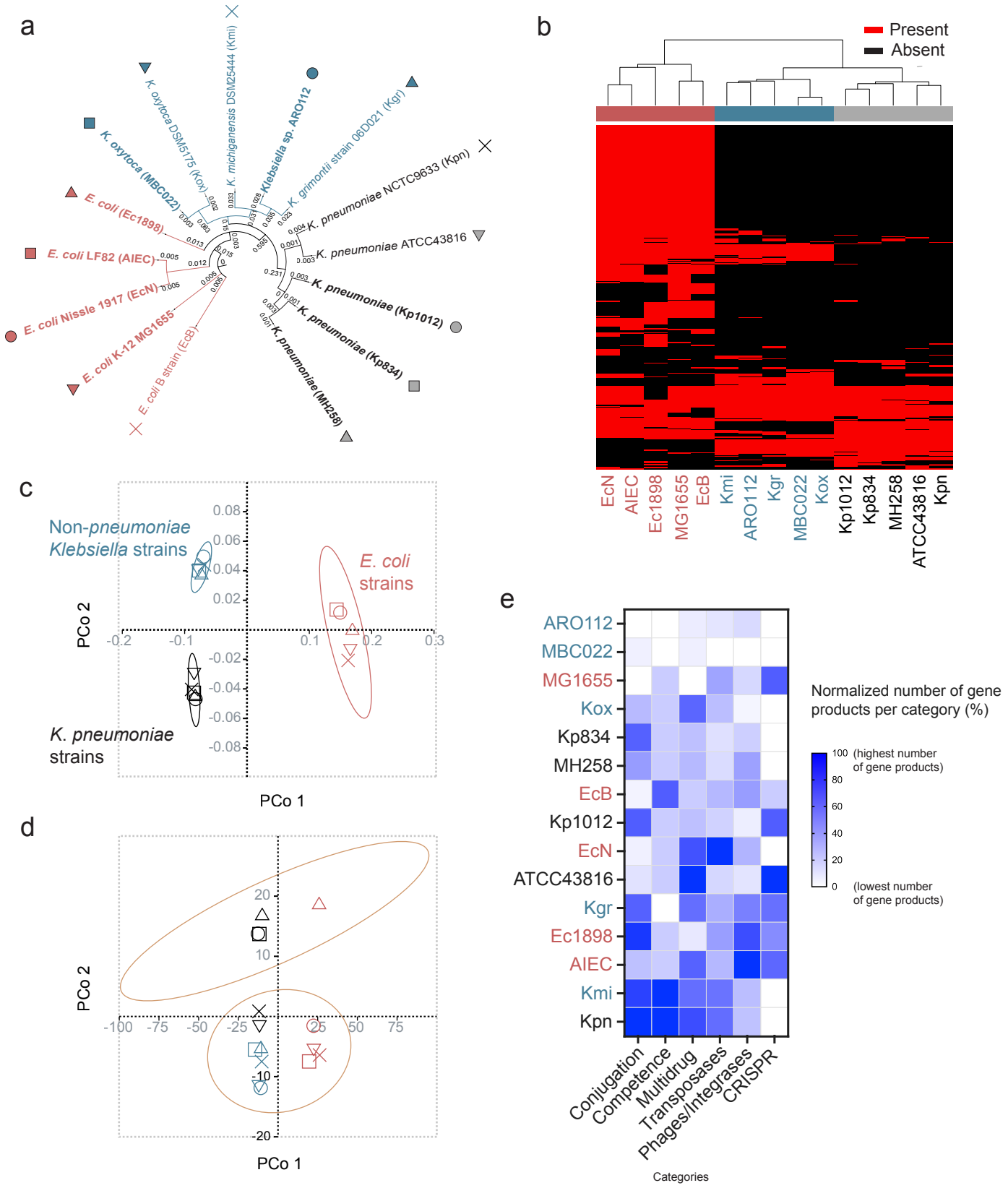
a
K. michiganensis DSM25444 (Kmi)
K. oxytoca DSM5175 (Kox)
Klebsiella sp. ARO112
K. grimontii strain 06D021 (Kgr)
K. oxytoca (MBC022)
K. pneumoniae NCTC9633 (Kpn)
E. coli (Ec1898)
K. pneumoniae ATCC43816
E. coli LF82 (AIEC)
K. pneumoniae (Kp1012)
E. coli Nissle 1917 (EcN)
E. coli K-12 MG1655
K. pneumoniae (Kp834)
E. coli B strain (EcB)
K. pneumoniae (MH258)
b
Present
Absent
EcN
AIEC
Ec1898
MG1655
EcB
Kmi
ARO112
Kgr
MBC022
Kox
Kp1012
Kp834
MH258
ATCC43816
Kpn
c
Non-pneumoniae Klebsiella strains
E. coli strains
K. pneumoniae strains
PCo 2
PCo 1
d
PCo 2
PCo 1
e
ARO112
MBC022
MG1655
Kox
Kp834
MH258
EcB
Kp1012
EcN
ATCC43816
Kgr
Ec1898
AIEC
Kmi
Kpn
Conjugation
Competence
Multidrug
Transposases
Phages/Integrases
CRISPR
Categories
Normalized number of gene products per category (%)
100 (highest number of gene products)
80
60
40
20
0 (lowest number of gene products)

Fig. 2

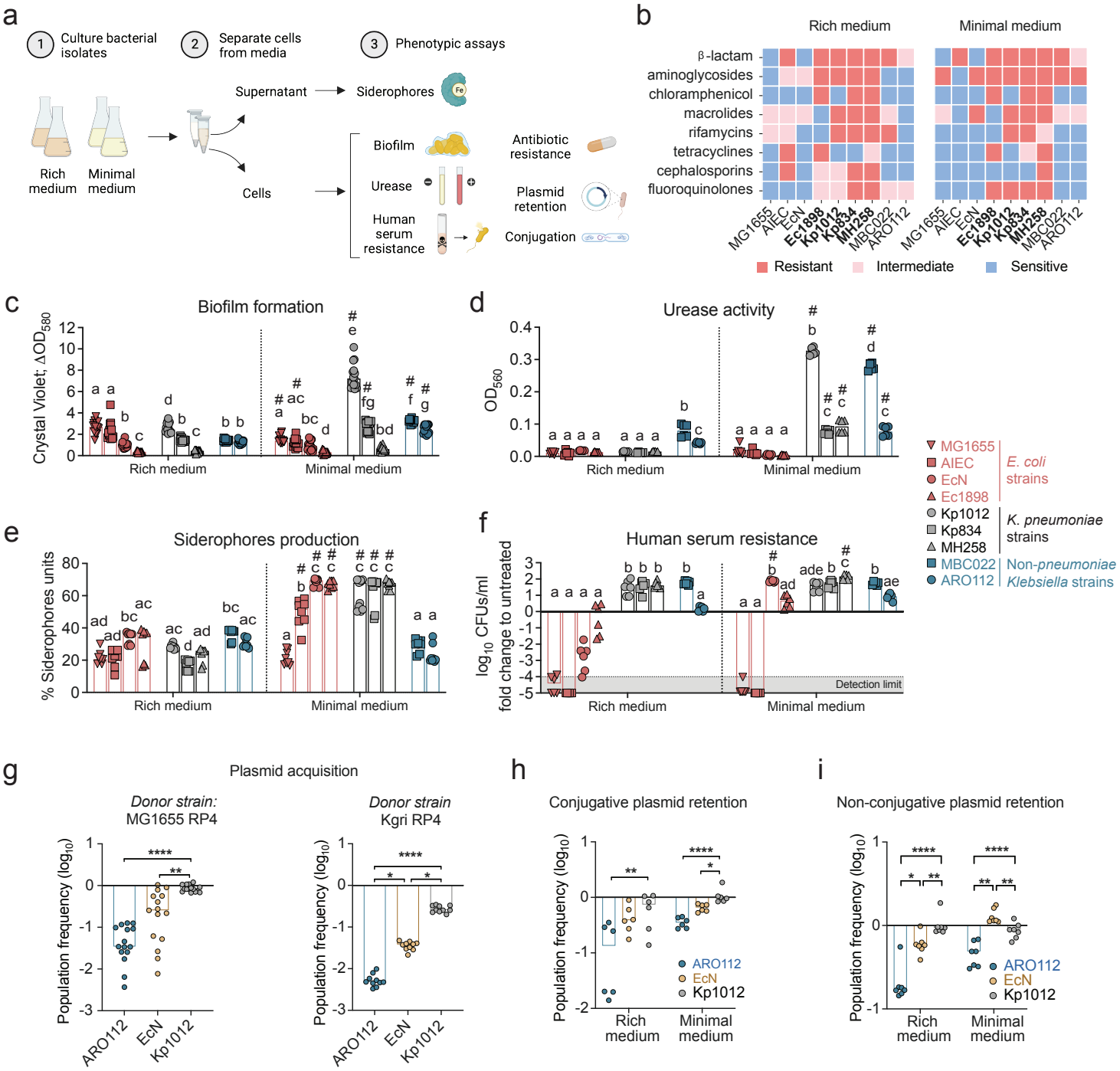
a
1 Culture bacterial isolates
2 Separate cells from media
3 Phenotypic assays
Rich medium
Minimal medium
Supernatant
Siderophores
Cells
Biofilm
Urease
Human serum resistance
Antibiotic resistance
Plasmid retention
Conjugation
b
Rich medium
Minimal medium
β-lactam
aminoglycosides
chloramphenicol
macrolides
rifamycins
tetracyclines
cephalosporins
fluoroquinolones
MG1655
AIEC
EcN
Ec1898
Kp1012
Kp834
MH258
MBC022
ARO112
Resistant
Intermediate
Sensitive
c
Biofilm formation
Crystal Violet, ΔOD580
Rich medium
Minimal medium
d
Urease activity
OD560
Rich medium
Minimal medium
MG1655
AIEC
EcN
Ec1898
E. coli strains
Kp1012
Kp834
MH258
K. pneumoniae strains
MBC022
ARO112
Non-pneumoniae Klebsiella strains
e
Siderophores production
% Siderophores units
Rich medium
Minimal medium
f
Human serum resistance
log10 CFUs/ml fold change to untreated
Detection limit
Rich medium
Minimal medium
g
Plasmid acquisition
Donor strain: MG1655 RP4
Donor strain Kgri RP4
Population frequency (log10)
ARO112
EcN
Kp1012
h
Conjugative plasmid retention
Population frequency (log10)
ARO112
EcN
Kp1012
Rich medium
Minimal medium
i
Non-conjugative plasmid retention
Population frequency (log10)
ARO112
EcN
Kp1012
Rich medium
Minimal medium

Fig. 3

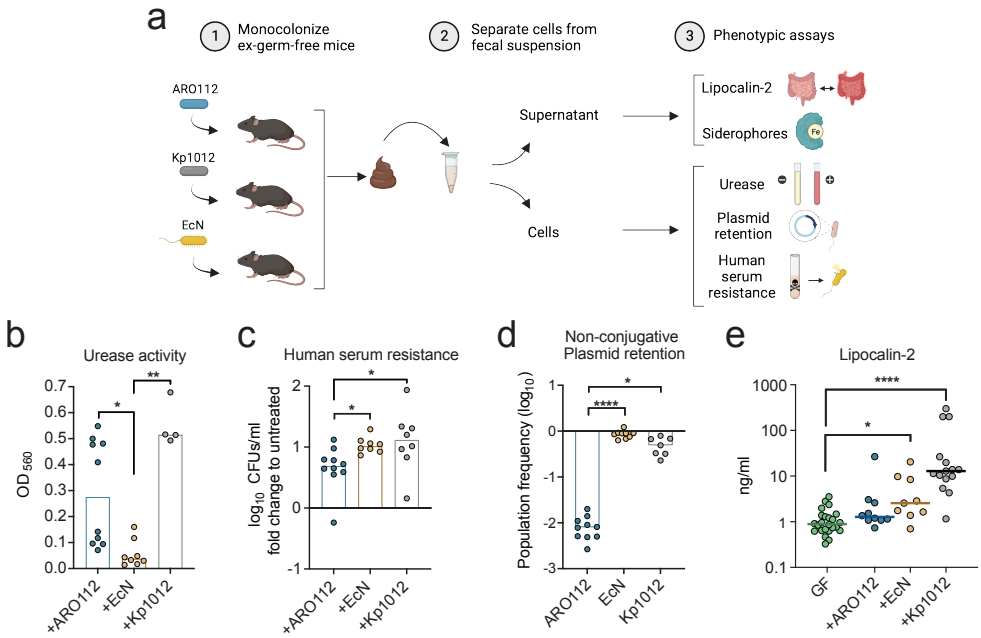
a
1 Monocolonize ex-germ-free mice
2 Separate cells from fecal suspension
3 Phenotypic assays
ARO112
Kp1012
EcN
Supernatant
Cells
Lipocalin-2
Siderophores
Urease
Plasmid retention
Human serum resistance
b
Urease activity
OD 560
+ARO112
+EcN
+Kp1012
c
Human serum resistance
log10 CFUs/ml fold change to untreated
+ARO112
+EcN
+Kp1012
d
Non-conjugative Plasmid retention
Population frequency (log10)
ARO112
EcN
Kp1012
e
Lipocalin-2
ng/ml
GF
+ARO112
+EcN
+Kp1012

Fig. 4

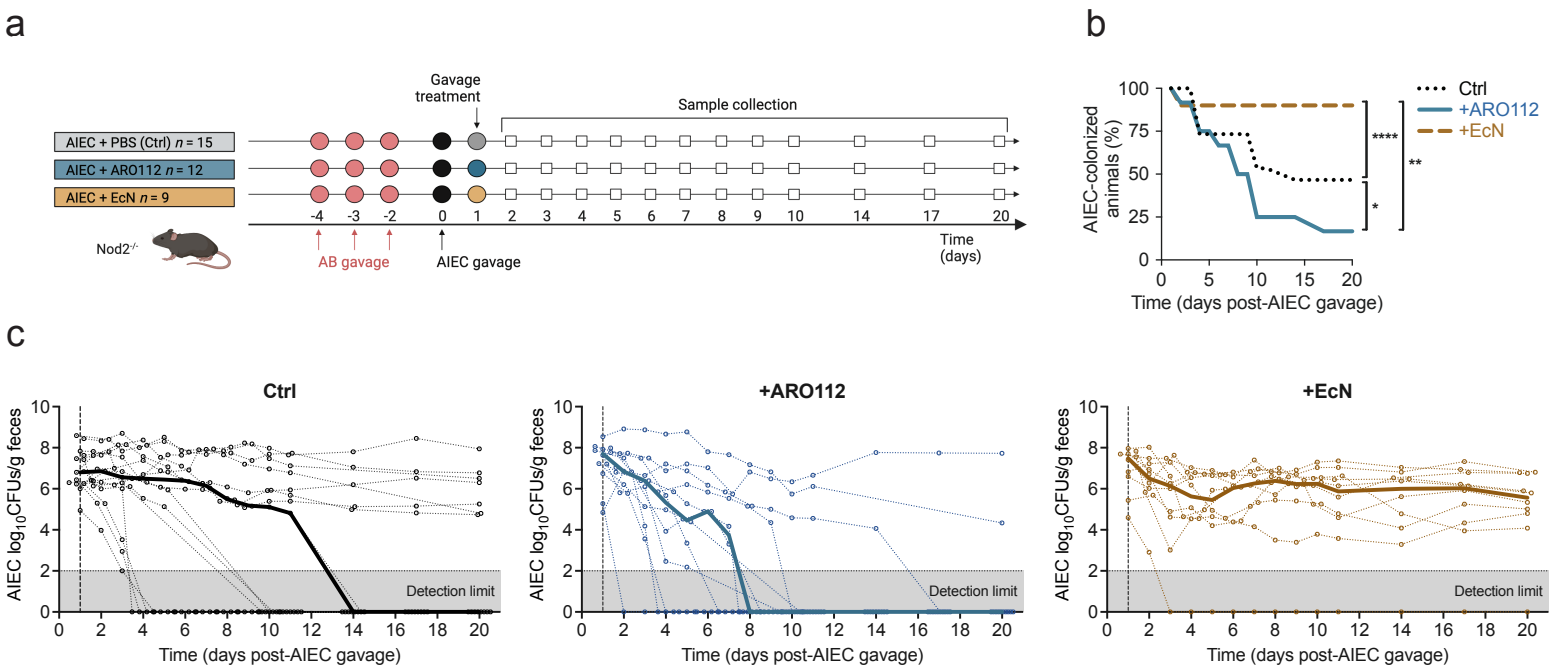
a
Gavage treatment
Sample collection
AIEC + PBS (Ctrl) n = 15
AIEC + ARO112 n = 12
AIEC + EcN n = 9
Nod2-/-
-4 -3 -2 0 1 2 3 4 5 6 7 8 9 10 14 17 20
AB gavage
AIEC gavage
Time (days)
b
AIEC-colonized animals (%)
Time (days post-AIEC gavage)
Ctrl
+ARO112
+EcN
****
**
*
c
Ctrl
+ARO112
+EcN
AIEC log10CFUs/g feces
Detection limit
Time (days post-AIEC gavage)

Fig. 5

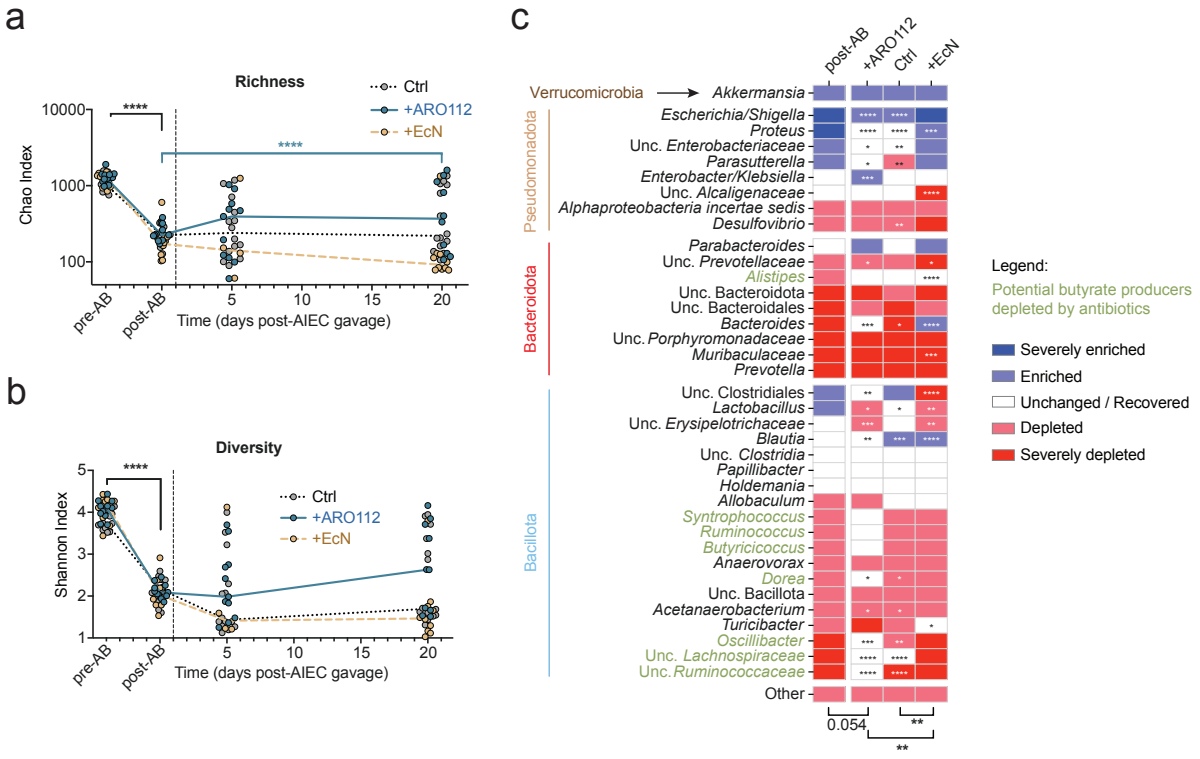
a
Richness
Ctrl
+ARO112
+EcN
Chao Index
10000
1000
100
****
****
pre-AB
post-AB
5
10
15
20
Time (days post-AIEC gavage)
b
Diversity
Shannon Index
5
4
3
2
1
****
Ctrl
+ARO112
+EcN
pre-AB
post-AB
5
10
15
20
Time (days post-AIEC gavage)
c
post-AB
+ARO112
Ctrl
+EcN
Verrucomicrobia
Akkermansia
Pseudomonadota
Escherichia/Shigella
Proteus
Unc. Enterobacteriaceae
Parasutterella
Enterobacter/Klebsiella
Unc. Alcaligenaceae
Alphaproteobacteria incertae sedis
Desulfovibrio
Bacteroidota
Parabacteroides
Unc. Prevotellaceae
Alistipes
Unc. Bacteroidota
Unc. Bacteroidales
Bacteroides
Unc. Porphyromonadaceae
Muribaculaceae
Prevotella
Bacillota
Unc. Clostridiales
Lactobacillus
Unc. Erysipelotrichaceae
Blautia
Unc. Clostridia
Papillibacter
Holdemania
Allobaculum
Syntrophococcus
Ruminococcus
Butyricicoccus
Anaerovorax
Dorea
Unc. Bacillota
Acetanaerobacterium
Turicibacter
Oscillibacter
Unc. Lachnospiraceae
Unc. Ruminococcaceae
Other
0.054
**
**
Legend:
Potential butyrate producers depleted by antibiotics
Severely enriched
Enriched
Unchanged / Recovered
Depleted
Severely depleted

Fig. 6

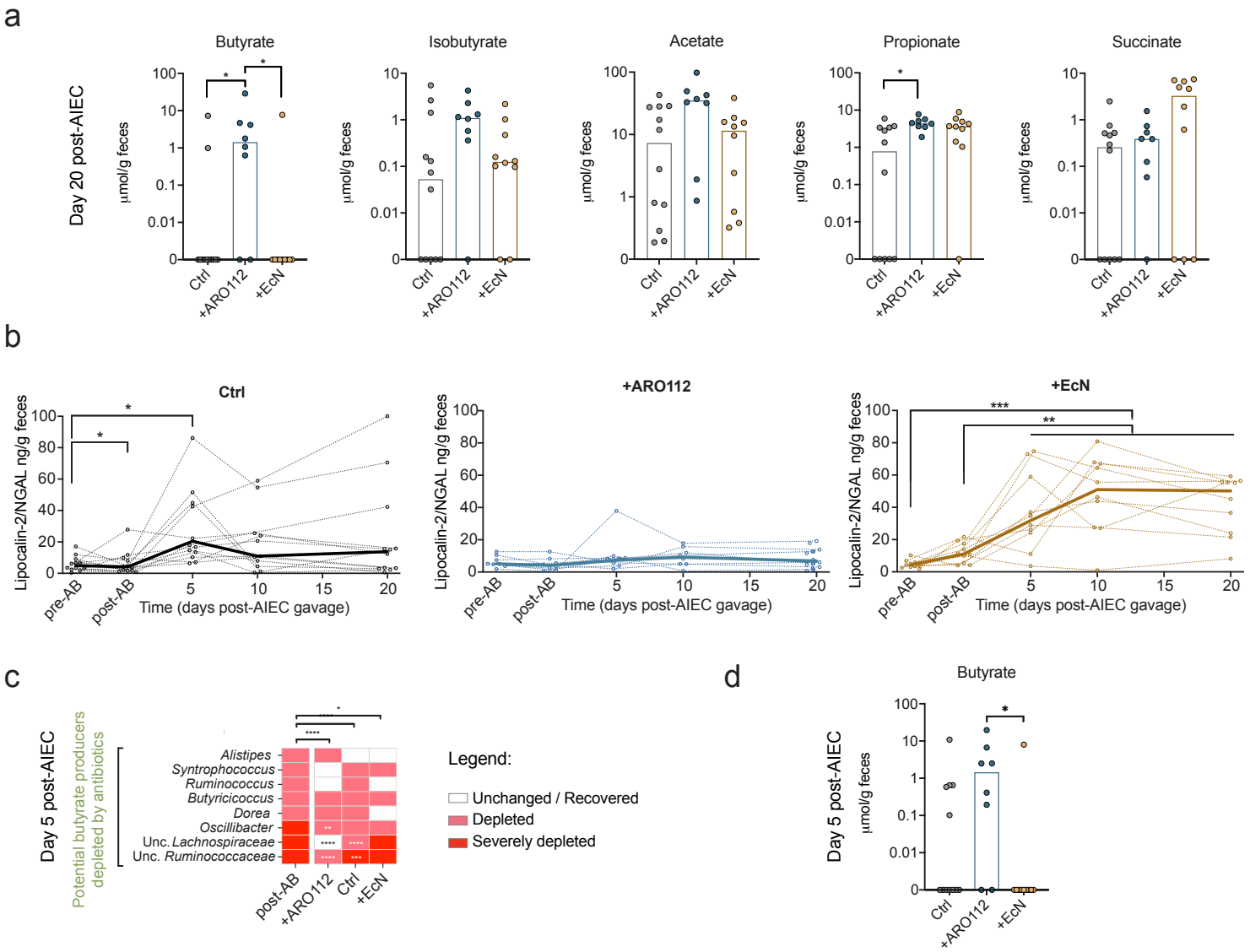
a
Butyrate
Isobutyrate
Acetate
Propionate
Succinate
Day 20 post-AIEC
µmol/g feces
Ctrl
+ARO112
+EcN
b
Ctrl
+ARO112
+EcN
Lipocalin-2/NGAL ng/g feces
pre-AB
post-AB
Time (days post-AIEC gavage)
c
Day 5 post-AIEC
Potential butyrate producers depleted by antibiotics
Alistipes
Syntrophococcus
Ruminococcus
Butyricicoccus
Dorea
Oscillibacter
Unc. Lachnospiraceae
Unc. Ruminococcaceae
post-AB
+ARO112
Ctrl
+EcN
Legend:
Unchanged / Recovered
Depleted
Severely depleted
d
Butyrate
Day 5 post-AIEC
µmol/g feces
Ctrl
+ARO112
+EcN